Surveys in Geophysics (2019) 40:1351–1397
https://doi.org/10.1007/s10712-019-09531-1

Forcing Factors Affecting Sea Level Changes at the Coast

Philip L. Woodworth[1] · Angélique Melet[2] · Marta Marcos[3,4] · Richard D. Ray[5] · Guy Wöppelmann[6] · Yoshi N. Sasaki[7] · Mauro Cirano[8] · Angela Hibbert[1] · John M. Huthnance[1] · Sebastià Monserrat[4] · Mark A. Merrifield[9]

Received: 30 September 2018 / Accepted: 4 April 2019 / Published online: 8 May 2019

Abstract
We review the characteristics of sea level variability at the coast focussing on how it differs from the variability in the nearby deep ocean. Sea level variability occurs on all timescales, with processes at higher frequencies tending to have a larger magnitude at the coast due to resonance and other dynamics. In the case of some processes, such as the tides, the presence of the coast and the shallow waters of the shelves results in the processes being considerably more complex than offshore. However, 'coastal variability' should not always be considered as 'short spatial scale variability' but can be the result of signals transmitted along the coast from 1000s km away. Fortunately, thanks to tide gauges being necessarily located at the coast, many aspects of coastal sea level variability can be claimed to be better understood than those in the deep ocean. Nevertheless, certain aspects of coastal variability remain under-researched, including how changes in some processes (e.g., wave setup, river runoff) may have contributed to the historical mean sea level records obtained from tide gauges which are now used routinely in large-scale climate research.

Keywords Coastal sea level variability · Sea and land level observations · Meteorological and oceanographic forcings · Coastal climate change

✉ Philip L. Woodworth
plw@noc.ac.uk

[1] National Oceanography Centre, 6 Brownlow Street, Liverpool L3 5DA, UK

[2] Mercator-Ocean, 31520 Ramonville Saint-Agne, France

[3] IMEDEA(UIB-CSIC), Miquel Marquès, 21, 07190 Esporles, Balearic Islands, Spain

[4] Department of Physics, University of the Balearic Islands, Cra. Valldemossa, km 7.5, 07122 Palma, Spain

[5] Code 698, NASA Goddard Space Flight Center, Greenbelt, MD 20771, USA

[6] LIENSs, Université de La Rochelle-CNRS, La Rochelle, France

[7] Science 8th Building, 8-3-20 Faculty of Science, Hokkaido University, N10, W8, Sapporo 060-0810, Japan

[8] Department of Meteorology, Institute of Geosciences, Federal University of Rio de Janeiro, Rio de Janeiro 21941-901, Brazil

[9] Scripps Institution of Oceanography, University of California, San Diego, La Jolla, CA 92093, USA

1 Introduction

Sea level variability at the coast can be similar to, or differ from, that in the neighbouring deep ocean, depending on location and timescale. For example, large spatial- and temporal-scale changes, such as a rise in mean sea level (MSL) due to climate change, might be expected to be similar, to first order at least, at the coast and in the ocean nearby.[1]

However, there are many processes which introduce sea level variability with shorter spatial scales, or which result in a coastal modification in the character of the larger-scale variability. These processes occur primarily due to coastal waters being shallow (by definition) and coastlines having complicated shapes and features such as estuaries and harbours. In addition, the coast provides one of the boundaries (the other being the continental shelf edge) which result in dynamical changes in the ocean circulation and thereby in the sea level variability observed over larger spatial scales. Runoff from rivers introduces another source of sea level variability from the landward side.

As one example, Fig. 1 (from Vinogradov and Ponte 2011) shows the correlation between monthly means of sea level measured at the coast by tide gauges and in the nearby ocean by satellite altimetry. The correlation is far from perfect and (leaving aside for the moment any questions of data imprecision) indicates that there are processes at work resulting in differences in sea level variability between coast and ocean, even on monthly timescales. This means that coastal processes need to be identified and understood as far as possible, partly so that they can be studied in their own right, and partly so that they can be clearly separated from the large-scale, climate-related signals.

In fact, there are many such coastal processes, operating at different timescales, for which in many cases the physics responsible is well understood. Many occur across the short spatial scales of the shelf (e.g., storm surges) or even shorter (e.g., harbour seiches), and timescales much shorter than the monthly and annual timescales of interest in climate studies. Others can occur on quite large spatial scales along the coast and on longer timescales. Examples include the trapped Kelvin waves along the Pacific coast associated with the El Niño–Southern Oscillation (ENSO) (Enfield and Allen 1980; Pugh and Woodworth 2014), or the long-distance correlations of sea level (or sub-surface pressure) along the shelf and slope (Hughes and Meredith 2006). Table 1 provides a list of such processes, while Fig. 2 demonstrates schematically the space and timescales of many of them.

The following sections of this paper discuss a number of forcing factors of coastal sea level variability. The first one refers to the tides, which are the dominant signal in sea level variability along all coastlines and which span a wide range of timescales. We then move to a discussion of a number of other processes, ordered approximately in terms of timescale instead of possible importance (magnitude), although sometimes processes again span different timescales, so the reader will have to be aware that such a division is not straightforward. We consider processes responsible for extreme sea levels, as well as MSL, extremes being of particular interest at the coast.

[1] Mean sea level (MSL) in altimetry usually refers to the average sea surface height at a point in the ocean over a period such as a month or year measured relative to a reference ellipsoid. MSL in tide gauge work is the average sea level measured by a tide gauge over a month or year relative to the height of a benchmark on the nearby land. The two types of MSL can be considered on the same basis when the height of the benchmark relative to the ellipsoid is measured using Global Navigation Satellite System (GNSS) equipment. Tide gauge MSL averaged over an extended period (traditionally 18.6 years) is often used as a national surveying datum. See Pugh and Woodworth (2014) and Gregory et al. (2019) for more detailed definitions of MSL.

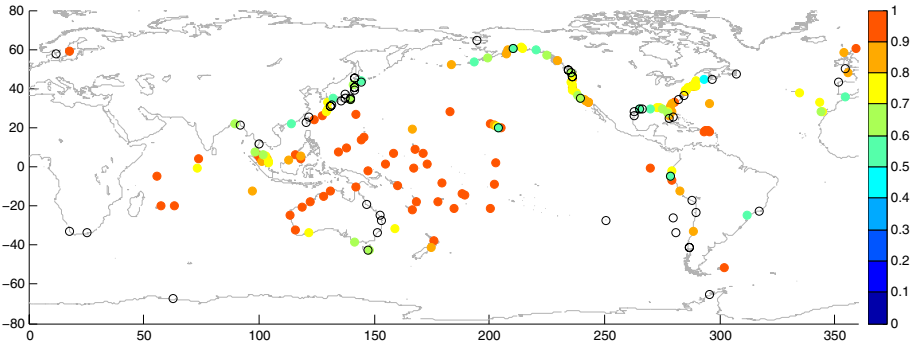

Fig. 1 Correlations between IB-corrected monthly mean sea levels measured at the coast by tide gauges and sea levels recorded by satellite altimetry in the nearby deep ocean over the period 1993–2008. Locations with correlations statistically indistinguishable from zero at 95% confidence level are shown as open circles. From Vinogradov and Ponte (2011)

However, it can be appreciated that, while there are many processes, there is only one ocean, so changes in depth introduced by one process necessarily introduce modifications to others. For example, there are interactions between tides and storm surges in coastal waters, due to both processes modifying the instantaneous depth. In addition, the generally deeper coastal waters arising from a rise in global MSL will result in an increase in tidal wavelengths and modification of patterns of tidal variability. Such interactions between processes are discussed in detail by Idier et al. (2019).

2 Tides

There is one topic that arises in a discussion of nearly every timescale: the tides (Pugh and Woodworth 2014). The dominant half-daily and daily periods of tidal variability are obvious, but tidal periods range from much shorter to very much longer than these. At shorter periods, compound tides such as M_4 (period 6.21 h) reach 25 cm at places like Dover, UK, and higher overtides such as M_{12} (2.07 h) or higher are often detectable and are sometimes even needed for precise predictions. At longer periods, the astronomical tides are all relatively small and sea level variability at these timescales is usually dominated by non-tidal processes, yet the impact of tides on long-term properties of extreme water levels can be pronounced; important tidal periodicities for extreme high water include fortnightly, 4.4 years and 18.6 years, and these will be referred to below. On even longer timescales, short period (semidiurnal and diurnal) tides are found to respond to long-term changes in the oceanic medium, seasonally in particular, but also at longer periods, even secular, leading to tentative connections between tides and climate.

Considerable progress has been made in recent years in modelling the tides of the deep ocean (Stammer et al. 2014), and Ray and Egbert (2017) have summarised major recent research progress in determining the energy budgets of the barotropic tides and in the transmission of internal tides across ocean basins (Zhao et al. 2016). Where internal tides break on a distant coast many days later, they can result in increased seiche activity on timescales typical of the shelf or harbour (e.g., Wijeratne et al. 2010).

Table 1 A highly schematic list of processes which contribute to sea level variability at the coast, in approximate order of timescale

	Process	Space scale	Magnitude	Comments	Example References
Waves and swell	Wind waves	1–10s km	10s cm to metres	Period 1–10 s	LeBlond and Mysak (1978)
	Ocean swell	10–100s km	Sometimes several metres	Period 10–20 s	LeBlond and Mysak (1978)
High frequency (min to hours)	Seiches	Harbour, Bay, Shelf-width, Basin	Typically decimetres, sometimes much larger (up to several metres) when externally forced by long waves (tsunamis or meteotsunamis)	Forced oscillations of variation in elevations and currents, usually forced by the wind, tide or breaking internal tide, or waves, or an impulse such as a tsunami or earthquake. Also generated importantly at the coast by the long waves of meteotsunamis	Monserrat et al. (2006). Rabinovich (2010). Wijeratne et al. (2010). Vilibić and Šepić (2017)
	Meteotsunamis	100s km in generation, harbour/bay scale in impact	Centimetric in the open ocean. 10s cm to potentially several metres after reaching the coast where associated harbour resonances are generated	Probably not appreciated as much as they should be as they need very high-frequency meteorological data to understand properly. Destructive when they amplify a seiche response by resonance	Monserrat et al. (2006). Rabinovich (2010)
High frequency to daily	Coastal trapped waves	100s to 1000s km alongshelf	Typically decimetres, sometimes metres as tidal Kelvin waves or storm surges	Coastal trapped waves underlie along-shelf propagation of responses to forcing. Scales (time, space, magnitude) depend on the forcing	Huthnance (2001). Hughes et al. (2019)
Daily	Tides	Basin scale in generation but more complex spatially in shallow water at the coast	Metres or 10s metres in shelf areas of resonance	Temporally and spatially complex tides in coastal waters	Ray et al. (2011). Ray and Egbert (2017). Pugh and Woodworth (2014)

Table 1 (continued)

	Process	Space scale	Magnitude	Comments	Example References
	Internal tides	Basin scale	Several cm	When break at the coast they can generate seiche activity	Ray and Egbert (2017)
	Inverse barometer	100s–1000s km synoptic weather scale	Decimetres and potentially ± 50 cm	1 cm change in sea level for 1 mbar change in air pressure (to within 0.5%). The ocean takes time to move so there is also a 'dynamic' air pressure change component on timescales of ~ 1 day	Wunsch and Stammer (1997). Discovery of IB effect described by Roden and Rossby (1999)
	Storm surges	100s km (shelf scale)	1–3 m or potentially ~ 10 m during extra-tropical and tropical cyclones, respectively	Generated by wind stress/water depth and air pressure according to the nonlinear shallow water (NLSW) equations	Gönnert et al. (2001). WMO (2011). Pugh and Woodworth (2014)
Examples of processes spanning timescales	Wave setup	Few 100 m for sloping beaches, harbour scales	Decimetres during a storm when high waves, potentially ~ 1 m in some harbours or lagoons	Contributes to MSL variability in the surf zone. Depends on offshore incident wave height, period, direction, still water level and on foreshore slope. Modulated over a range of timescales	Thompson and Hamon (1980). Stockdon et al. (2006). Dean and Walton (2009). Vetter et al. (2010). Aucun et al. (2012), Becker et al. (2014)

Table 1 (continued)

	Process	Space scale	Magnitude	Comments	Example References
	Swash and wave runup	As for setup	Zero contribution to mean sea level in that mean swash is zero and mean runup is equal to the setup	Oscillatory contribution. Depends on offshore incident wave height, period, direction, still water level and on foreshore slope. Large factor in coastal flooding and in shaping coastlines	Stockdon et al. (2006). Roelvink et al. (2009). Kennedy et al. (2016). Poate et al. (2016)
	River runoff	10–100 km (or even larger for the Amazon)	Several cm for most rivers. Major contribution to MSL seasonal cycle in large deltas.	Largely neglected (so far) contributor to sea level variability on timescales other than seasonal	Meade and Emery (1971). Laiz et al. (2014). Wijeratne et al. (2008). Piecuch et al. (2018)
Seasonal	Steric changes	Basin or shelf-scale	Decimetres	Due to seasonal expansion/contraction of the water column	Gill (1982)
	Met changes	Shelf scale	Decimetres	Due to seasonal cycles in air pressure, winds, runoff, etc.	Vinogradov and Ponte (2010)
	Upwelling/downwelling	100s km	Decimetres	Due to seasonal variations in local winds	Middleton and Cirano (1999). Middleton (2000)
	Tides	Shelf-scale	Centimetric	The main tidal harmonics have small seasonal sidebands in the tidal potential. However, on shelves they can vary annually by a much larger amount (typically 1%) due to shelf processes	Pugh and Vassie (1976, 1992). Müller (2012). Gräwe et al. (2014)

Table 1 (continued)

	Process	Space scale	Magnitude	Comments	Example References
	Extremes	Shelf-scale	Decimetres to potentially a metre	Obvious seasonal cycle in sea level extremes due to the weather	Menéndez and Woodworth (2010)
Interannual	ENSO, NAO, etc.	Largely basin scale although with some global teleconnections	Decimetres	In addition to contributing to MSL directly, an impact on mean offshore wave conditions (height, direction, period) and hence setup	Stopa and Cheung (2014). Han et al. (2017a,b, 2018a,b)
Decadal and internal variability	PDO, IOD, etc.	Basin scale	Decimetres	Primarily large scale rather than coastal scale, but there can be associated impacts on coastal processes	Han et al. (2014, 2017a, b, 2018a, b)
Ocean dynamics	Western Boundary Currents	100s km	Decimetres	The coast acts as a low-pass filter for sea level change in the nearby ocean	Bingham and Hughes (2009). Sallenger et al. (2012). Boon (2012). Yin and Goddard (2013). Higginson et al. (2015)
	Eastern coastal currents	1000s km along-shelf, 100 km cross-shelf	Sub-decimetric	Depends on along-shore coastal wind stress	Calafat et al. (2012)
	Coherent variability in SSP along continental shelf and slope	1000s km along continental shelf and slope	Mostly centimetric	Observed in altimeter data and confirmed by models	Hughes and Meredith (2006)
	Mesoscale (eddies, Rossby waves) at ocean islands	~ 100 km and ~ 10 day timescale	Decimetres	Observed in some island sea level records	Mitchum (1995). Williams and Hughes (2013)

Table 1 (continued)

	Process	Space scale	Magnitude	Comments	Example References
Long-term/climate change	Sea level rise	Global although regional variations. Associated changes in water depth (relative sea level) will depend on regional vertical land movements	Decimetres to metre or so by 2100	Changes in water depth modify tides, surges and waves (see Idier et al., 2019). Changes in winds in response to climate change induce changes in mean offshore wave conditions, including height, direction and period, which in turn induce changes in wave setup and runup	Church et al. (2013)
	Tides	Global/regional/local	Secular changes in tidal constituents of order 0.1% in amplitude have been observed that are not well understood	Changes in tides in the future will depend on changes in depth (MSL) from other processes, changes in thermal structure of the water column, etc.	Jay (2009), Ray (2009), Woodworth (2010), Müller et al. (2011), Haigh et al. (2019)
Vertical land movements	Change in the level of the crust (submergence or emergence) relative to the geocentre	Global scale for Global Isostatic Adjustment (GIA). Local scale for natural causes such as earthquakes and a number of anthropogenic factors	Decimetres to metres or so by 2100	GIA is only process that can be modelled on a global basis	Tamisiea and Mitrovica (2011). Peltier et al. (2015). Wöppelmann and Marcos (2016)
Anthropogenic factors					See text

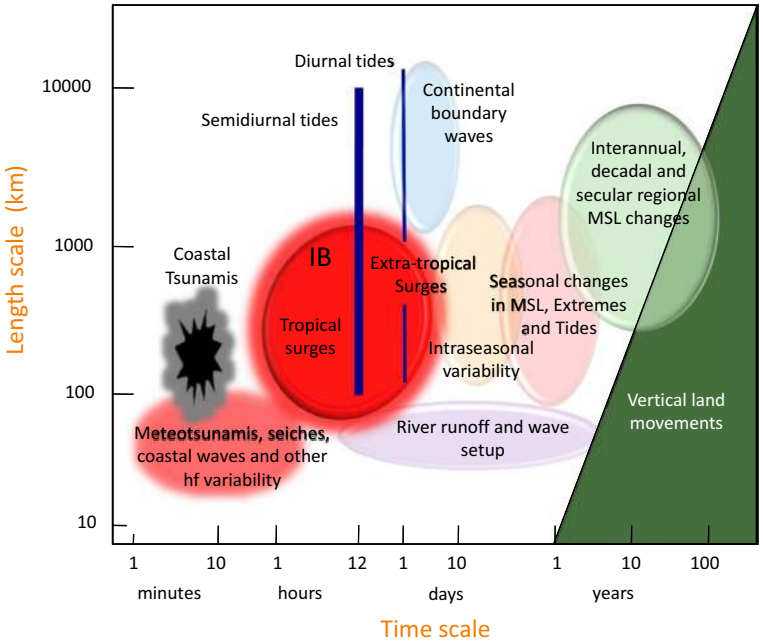

Fig. 2 A schematic overview of processes contributing to sea level variability at the coast indicating the space and timescales involved. Note that Table 1 contains a fuller list of processes than those shown here. Very high frequency processes with timescales less than 1 min (wind waves, swash, etc.) are not included. See Hughes et al. (2019) for a detailed review of different types of coastal trapped waves

The ocean tides are largely generated in the deep ocean. However, their transition to the shelves and to the coast results in their amplification, partly through resonance depending on the shape of the coast and depth of coastal waters, and the generation of higher harmonics of their main frequencies. As a result, many difficulties remain in parameterising the more complex tides which occur near the coast (Ray et al. 2011). Figure 3a provides a demonstration of the complexity of the tide at one coastal location (Eastport, Maine, NE USA). The main semidiurnal and diurnal lines to the left of the spectrum, and a number of others, are now represented well in global ocean tide models (e.g., FES2014 2018). However, it can be appreciated that a major challenge remains to parameterise spatially the many harmonics at frequencies higher than 2 cpd, and also the subtleties of variability and interaction hidden within the tidal cusps.

Figure 3b provides a contrasting spectrum obtained from a bottom pressure (BP) sensor on a Deep-ocean Assessment and Reporting of Tsunami (DART) buoy deployed at 2600 m depth just south of the New England shelf. Although the main semidiurnal and diurnal tides have similar amplitudes to those at Eastport, the higher tidal harmonics are either considerably weaker or absent, those at 5, 7 and 9 cpd in (b) being due to atmospheric tides in BP and not oceanic tides. One may also note the lower non-tidal background provided by a BP record compared to the sea level record of a conventional coastal tide gauge.

One subtlety to do with tidal variability concerns the apparent long-term changes in tidal amplitudes and phases along the coast; it is not yet known whether similar changes are occurring in the deep ocean. Of course, the tide changes over long timescales in response

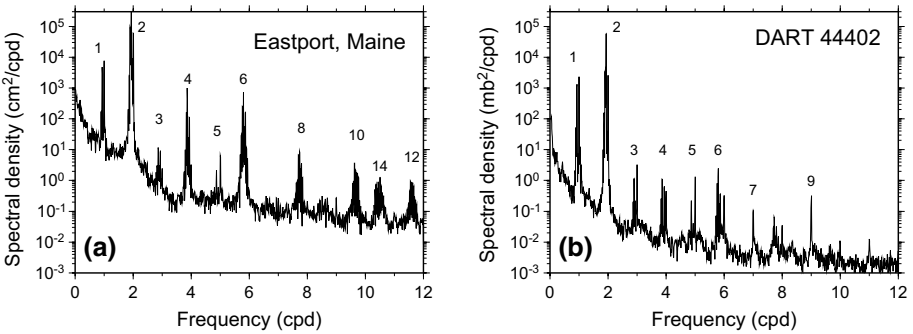

Fig. 3 **a** A sea level spectrum from Eastport, Maine, on the US NE Atlantic coast, highlighting the main tidal band. The dominant tidal constituent is the lunar semidiurnal M_2, but strong nonlinear compound tides appear at higher frequencies. Numerical labels denote tidal species, where each species n consists of multiple spectral lines clustering around n cycles per lunar day. The spectrum is obtained from four years of hourly spot readings from the Eastport tide gauge. The Nyquist frequency is therefore 12 cpd, so species 14 is aliased into lower frequencies. **b** The corresponding spectrum of bottom pressure (BP) obtained from a nearby deep-ocean buoy (2600 m depth, south of the New England shelf). The higher oceanic tide harmonics are much reduced, the peaks at 5, 7 and 9 cpd being due to atmospheric tides in the BP record

to changes in the orbit of the Moon (Green et al. 2017), and when coastlines and water depths change. However, the presently observed tidal changes (mostly during the past half-century) cannot be explained by simple arguments and constitute an important topic in tidal research (Hill 2016; Haigh et al. 2019).

3 High-Frequency to Daily Coastal Variability

Sub-daily oscillations of sea level near the coast are strongly controlled by bathymetry and local topography. Seiches provide examples of such oscillations. Seiches are a type of resonance in which the sea level oscillates at a natural period of an inlet, harbour, bay or continental shelf (Rabinovich 2010). They were observed first in lakes (Forel 1876) and have since been found to be present in almost all tide gauge records (e.g., Airy 1878). Even larger bodies of water such as the Adriatic Sea and Baltic experience seiches (Lisitzin 1974).

The physical characteristics of a seiche in a lake can be considered similar to that of a guitar string tied at both ends (i.e. a node at each end), while a seiche in a semi-enclosed basin such as a coastal inlet is analogous to a string tied (i.e. a node) at only one of its ends. Resonances can therefore occur with wavelengths twice the lake length in the former case, or four times the inlet length in the latter. Similarly, 'quarter-wavelength seiches' occur across continental shelves, with a node at the land end and an anti-node at the shelf edge. The frequency of a seiche is then given by its wavelength divided by $\sqrt{gh}$ where g is acceleration due to gravity and h is water depth. In the case of complicated coastal geometries, additional factors also play a role (Rabinovich 2010; Wiegel 1964; Wilson 1972).

Free oscillations of a natural system (their so-called natural resonant periods or 'eigenperiods') occur as a response to any external input of energy. In the case of coastal seiches, the forcing is normally in the form of long waves entering through the coastal basin mouth. These periods may be considered as a fundamental property of a particular location and are independent of the type of external forcing (see below). Natural basins generally oscillate

with periods ranging between a few minutes and several hours, with amplitudes of centimetres to decimetres. However, at some locations and in some circumstances seiches can have amplitudes comparable to the tide. A maximum response will occur when an external forcing impinges on a basin mouth with a frequency corresponding to its eigen-frequencies. Seiche amplitudes may be then strongly amplified, and the currents associated with them and the resulting flooding inside the basin may cause serious damage to boats and harbour infrastructure. This is particularly the case when the amplification at resonance, characterised by the so-called quality factor Q, is particularly high. In basins with a high Q, generally those that are elongated and narrow, high levels of background seiche energy are also more likely to be present, even with a low level of external forcing (Rabinovich 2010).

There are several processes in nature which are able to generate oceanic long waves with periods matching the eigen-periods of basins and which are able to force them resonantly. Amongst them, tsunamis are probably the best-known phenomena. Tsunami wave properties are determined by the characteristics of the sea floor displacements (earthquakes) which generate them. They propagate as surface long waves with typical wavelengths of hundreds of kilometres and wave periods of up to an hour. The most energetic events affect the coast indiscriminately. However, less energetic tsunamis can also have a major impact where seiche frequencies match those of the tsunami itself, when a resonant coupling takes place and a seiche response is amplified at the local eigen-frequencies. As a consequence, there can be catastrophic consequences for harbours and bays with high Q-factors (Miller 1972; Rabinovich 1997; Rabinovich and Thomson 2007).

Seiches may also be forced by a number of other mechanisms, the most common processes being of atmospheric origin, either due to direct generation of long waves by pressure or wind forcing on the sea surface, or by transferring energy from low-frequency motions (storm surges) or high-frequency gravity waves (wind waves and swell) through nonlinear processes. The first mechanism is the most important because it is responsible for the generation of destructive seiche oscillations (meteotsunamis) all around the world (Defant 1961; Rabinovich and Monserrat 1996; Monserrat et al. 2006).

Destructive meteotsunamis are observed at certain locations in the world ocean where two mechanisms play a successive role: (1) the initial atmospheric energy is optimally transferred into the ocean through some specific resonant process, namely Proudman resonance (when atmospheric disturbance velocity equals the long wave phase speed of the ocean waves), Greenspan resonance (when atmospheric velocity matches that of edge wave modes, see below) or shelf resonance (when the atmospheric disturbance and associated generated ocean wave have periods and/or wavelengths equal to the resonant values for the shelf region); and (2) the generated long ocean waves approach the entrance of a bay or harbour and induce hazardous oscillations in the basin, exciting the basin seiche through harbour resonance (Monserrat et al. 2006).

Vilibić and Šepić (2017) demonstrated that many tide gauge records contain high-frequency variability on timescales from a few minutes to 2 h, which will include any energy due to seiches, although will not necessarily be exclusively due to seiches. They showed that such high-frequency variability, which is often not considered in studies of extreme sea levels based on hourly values from tide gauges, can contribute up to 50% of sea level extremes in some low-tidal areas.

Other high-frequency sea level oscillations can occur at the coast due to existence of the continental shelf, with the shelf characteristics (width and depth) playing a key role in determining their properties. For example, there are waves that travel along the coast or shelf and decay away from the coast: these include edge waves (periods of minutes to hours) and coastal trapped waves. The latter term usually applies to waves with periods

longer than an inertial period and is at least partially dependent on the Earth's rotation and vorticity dynamics. A summary of their properties may be found in Huthnance (1978), Huthnance et al. (1986), Huthnance (2001) and references therein. Kelvin waves, with an elevation maximum at the coast and the greatest offshore extent (no offshore nodes of elevation), span the frequency range from edge waves (super-inertial) to coastal trapped waves (sub-inertial). (A 'mode-0' barotropic Kelvin wave in an idealised (straight shelf) context can propagate at super-inertial frequencies without losing energy, as can internal Kelvin waves against a wall. Stratification makes little difference to the mode-0 Kelvin wave. Edge waves are exclusively super-inertial.)

The temporal and spatial scales of these waves depend mainly on the forcing (tides, weather, adjacent oceanic features) and the width of the continental shelf or slope, and on stratification for baroclinic waves. Modes with scales best matching the forcing tend to be favoured. Thus, tides propagating as Kelvin waves may have an amplitude of metres (e.g., Pugh and Woodworth 2014), while amplitudes of coastal trapped wave components are more typically 0.1 m. For example, weather- and oceanic-forced coastal trapped waves have magnitudes of typically 0.1 m, but extreme storm surges may be ± 1 m or more (e.g., Gönnert et al. 2001; Merrifield et al. 2013).

Hughes et al. (2019) discuss further the physical mechanisms for generation, propagation and decay of coastal trapped waves and their role in determining differences in sea level between deep-ocean, shelf and coast and in transmitting dynamical signals rapidly around the ocean.

4 Daily Coastal Sea Level Variability

In this section, we refer to several types of processes with meteorological forcing which result in sea level variability on timescales of several hours to several days (which we denote as 'daily'). Some of these are well known and are described adequately in text books.

One of the most important meteorological forcings of sea level variability over the open ocean, as well near the coast, is variability in surface air pressure. The inverse barometer (IB) effect, whereby an increase of 1 mbar in air pressure results in approximately 1 cm decrease in sea level (to within approximately half a per cent), was discovered in Sweden by Nils Gissler (Roden and Rossby 1999). An historical example of the IB effect using data collected in 1842 is given in Fig. 4. Other historical examples from the early nineteenth century are discussed by Daussy (1831), Lubbock (1836) and Ross (1854). As the ocean takes some time to adjust to a new equilibrium (typically ~ 1 day), there is a transient 'dynamic air pressure effect' (e.g., Ponte et al. 1991). Within the spectrum of air pressure variability in some parts of the ocean, and consequently within that of sea level variability, are modes with particular periods. These include the Madden–Julian 5-day waves which are, in principle, global in scale but are most evident in the tropics where the overall magnitude of air pressure variability is less (Luther 1982; Woodworth et al. 1995). (These are not to be confused with the approximately 4-day equatorial-trapped waves discussed by Wunsch and Gill 1976.)

Wind stress is the shear force that the wind exerts on the ocean surface and is proportional to the square of the wind speed (Pugh and Woodworth 2014). Wind stress is a relatively more important forcing of sea level variability than air pressure in shallow-water areas, where increases in sea level gradients are proportional to wind stress divided by

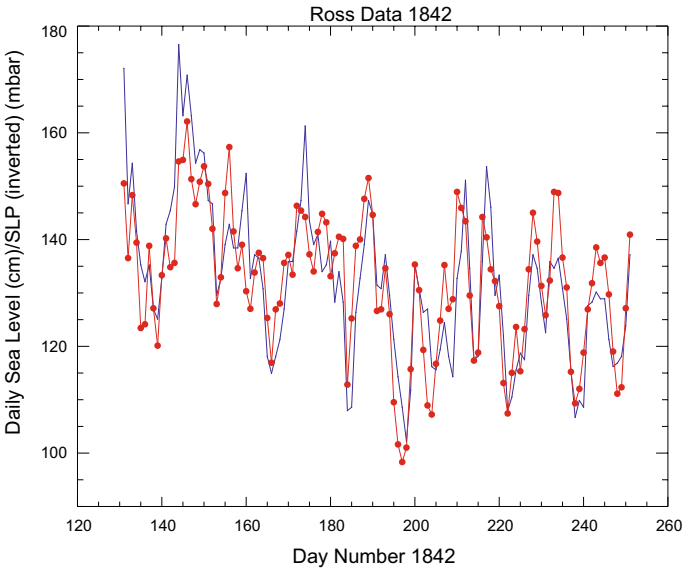

Fig. 4 Historical demonstration of the IB effect. Daily values of sea level (i.e. mean tide level, MTL) in 1842 at Port Louis, Falkland Islands (blue) together with daily values of sea level air pressure (SLP) (red), both measured by James Clark Ross. Air pressure values are shown inverted and their average adjusted to equal that in MTL. The MTL daily values are defined as the average of the average of high waters and average of low waters recorded each day. From Woodworth et al. (2010)

water depth. In addition, the coastal boundary acts to block wind-driven transport, leading to sea level elevation at the coast. As a result, coastal sea level variability on daily to monthly timescales departs significantly from an IB response to air pressure change (e.g., for the east coast of the UK, Thompson 1980; Woodworth 2018).

At times, the sea level changes resulting from a combination of air pressures and winds, called storm surges, can result in catastrophic flooding and loss of life. Depth-averaged (or barotropic) tides and storm surges can be modelled using the depth-averaged (2D) nonlinear shallow-water (NLSW) equations (Gönnert et al. 2001; WMO 2011; Pugh and Woodworth 2014; Piecuch et al. 2019). Such modelling schemes are used operationally in many countries (Flather 2000) and can be employed in delayed mode in research studies of coastal sea level variability (Carrère and Lyard 2003; Wakelin et al. 2003) and sea level extremes (Muis et al. 2016). Tides, winds and waves can also energise seiches (quasi-resonant modes of oscillation of sea level in inlets, bays, harbours and shelves, see Sect. 3) that can be superimposed on a storm surge and can consequently result in a higher measured extreme sea level.

An insight into waves is important for simulating accurately the daily variations in sea level in numerical models. Bottom friction coefficients used in barotropic modelling have been shown to depend on wave height (Madsen et al. 1988; Wolf 1999; Soulsby and Clarke 2005), although in practice such dependence is not usually taken into account. Nevertheless, this provides a further example of interaction between processes (tide-surge-wave) discussed by Idier et al. (2019).

The storm surges caused by tropical cyclones are different in character to those produced by higher latitude storms. Tropical storm surges tend to be of smaller spatial scale (~ 500 km rather than ~ 1000 km) and usually have a shorter duration (hours to days rather

than several days), but are much larger in amplitude (sometimes 5–10 m rather than typically 2–3 m) (von Storch and Woth 2008). Extreme sea levels occur by the combination of surge and astronomical tide and clearly have their most extreme values when both tide and surge are large and coincide. Extreme sea levels are usually studied by techniques such as percentile analysis (Menéndez and Woodworth 2010). In strongly semi-diurnal tide regimes, the high percentiles have a perigean (~4.4 year) dependence, while in strongly diurnal tide regimes the high percentiles vary over the lunar nodal cycle (18.6 years) (Haigh et al. 2011).

Merrifield et al. (2013) made maps of mean annual maximum sea level (relative to annual mean MSL, thereby excluding consideration of interannual variability) at many locations round the world coastline, and also maps of the individual contributions to mean annual maximum sea level from either the tide, seasonal cycle in sea level or low and high-frequency variations. The low-frequency components were defined by timescales longer than approximately a month but less than seasonal, whereas high-frequency variations were identified using a running 1-month median filter. Mean annual maximum levels occur where tide and low-frequency components are both large, such as the coasts of the North East Pacific, North West European continental shelf and North West Australia, while high-frequency variability was shown to be relatively more important along the American Atlantic coast and in North West Europe and South Australia (see their Figs. 3, 4).

One concern arises from the fact that the largest extremes (and so the events with the most catastrophic flooding) might not be represented adequately in tide gauge data sets. This reservation applies particularly to extremes caused by tropical storms. By definition, these events are rare ones and, when they do occur, the highest sea level may not be located exactly at the gauge, but some distance away. Therefore, this type of event may not be sampled adequately, even in a record spanning many decades. Furthermore, some gauges may not be able to record very high sea levels, and during an energetic storm, a gauge might be destroyed and so the extreme may not be recorded. To some extent, this is a sampling issue that can be addressed by analysing the tide gauge data in combination with numerical ocean modelling (e.g., Haigh et al. 2014a, b).

Changes in MSL are a major driver of changes in extreme sea levels at interannual and longer timescales (Lowe et al. 2010; Menéndez and Woodworth 2010; Woodworth et al. 2011; Marcos and Woodworth 2017, 2018). For example, Fig. 5 shows that linear trends of annual 99th percentiles of total sea level since 1960 (these are a good approximation of annual extreme levels), and of skew surges over the same period, can be accounted for to a great extent by trends in MSL. However, MSL is not the only driver: analyses of high-frequency tide gauge records, once the effect of MSL has been removed, reveal variations in the storm surge contribution associated with changes in storminess on long timescales (Menéndez and Woodworth 2010; Marcos et al. 2015; Marcos and Woodworth 2017). The intensity and frequency of storm surge changes unrelated to MSL show regionally coherent patterns that have been linked to large-scale climate indices, such as the North Atlantic Oscillation (NAO) in the North Atlantic (Marcos et al. 2015; Wahl and Chambers 2015; Marcos and Woodworth 2017). Similar conclusions on MSL being a major, if not the only, driver of changes in extremes were obtained using a small number of very long tide gauge records starting in the mid-nineteenth century.

Semidiurnal and diurnal variations in meteorological forcings that can potentially lead to sea level variability are of particular interest in the tropics. For example, air pressure has a predominantly semidiurnal cycle throughout the tropics (Pugh and Woodworth 2014, Sect. 5.5), with an amplitude of more than 1 mbar, peaking at about 10:00 and 22:00 h local time. Small diurnal variations in wind speed occur in the synoptic trades (e.g., in

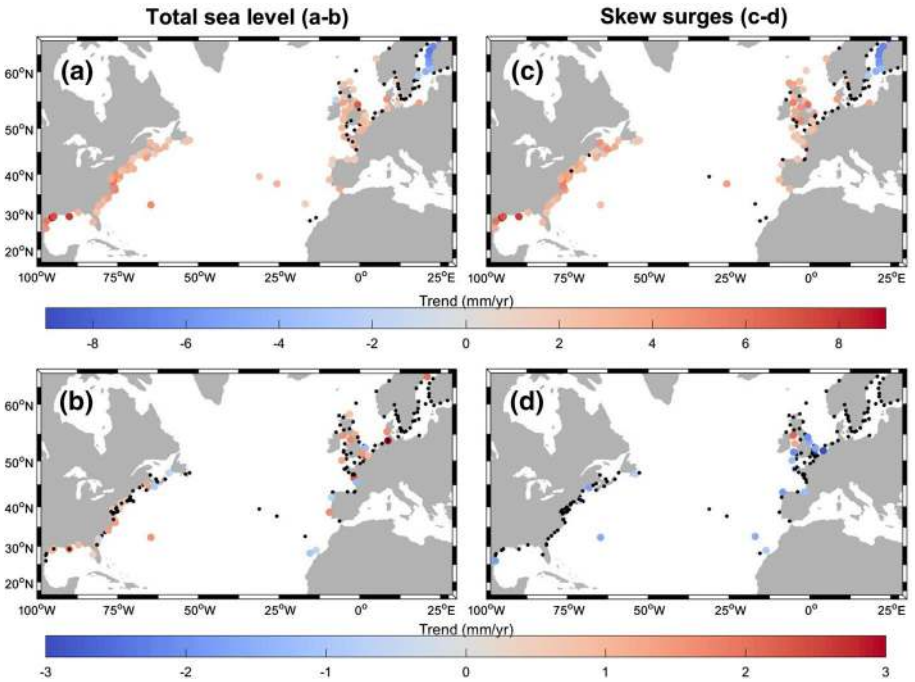

Fig. 5 **a** Linear trends of annual 99th percentiles of total sea level and **b** with median removed. **c** Linear trends of annual 99th percentiles of skew surges and **d** with median removed. Tide gauge data from 1960 to present are used. Black dots indicate where the trends are not significant. From Marcos and Woodworth (2018)

the Caribbean, Cook and Vizy 2010) and are best measured in situ by ocean buoys well away from land. However, much larger diurnal cycles in wind speed are found in data from some coastal land stations. These occur due to local sea and land breeze effects, which at locations in the tropics can extend 10s of km from the coast (Miller et al. 2003; Gille et al. 2005), and can affect many physical and biological processes including the local ocean circulation (e.g., Walter et al. 2017) and conceivably sea level to some extent. Inevitably, the sea and land breezes are not represented well in the large-scale meteorological products that are used for storm surge modelling.

5 Examples of Processes Spanning Timescales

As a demonstration of the difficulty of drawing simple diagrams such as Fig. 2, with some processes spanning a range of timescales, this section considers the importance to sea level studies of ocean waves. Waves manifest themselves at the high-energy end of the instantaneous sea level spectrum, and yet it will be seen that through long-term changes in wave climate waves can also contribute to long-term changes in MSL. This section also considers river runoff as a further example of processes spanning timescales that can contribute to MSL variability.

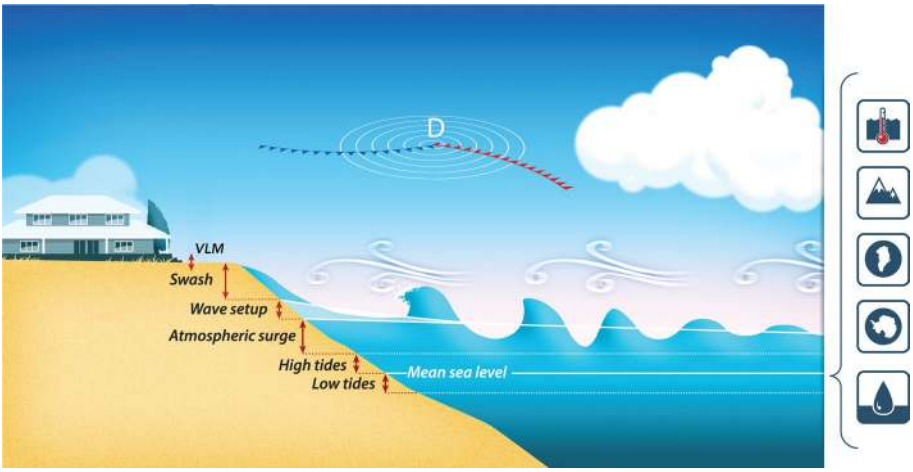

Fig. 6 Schematic of processes contributing to total water level changes at the coast. The mean sea level derived from radar altimetry data includes contributions from ocean thermal expansion and ocean circulation, transfer of water from land to ocean due to mass loss from glaciers and the Arctic and Antarctic ice sheets, as well as from land water storage changes (pictograms on the right, top to bottom). Sea level variability from tides and coastal processes including storm surges due to air pressure effects and wind setup, as well as wave setup and swash are superimposed on the larger-scale changes. Vertical land movements are denoted by VLM. The rotation of the depression (D) applies to the northern hemisphere. Adapted from Melet et al. (2018)

5.1 Wave Setup

Tides, surges and MSL together make up the 'still water level' superimposed upon which there are ocean wind waves. Wind waves span a range of period typically 1–25 s (LeBlond and Mysak 1978). The wave field impinging on a given location at the coast is usually composed of waves of different origins, ages and periods. Part of that field will consist of locally generated waves with shorter periods, while waves with longer periods will partly comprise ocean swell that could have travelled 1000s of km from distant storms (Ardhuin et al. 2009). Distantly generated swell has been found to result in major impacts on coastlines far from its generation (e.g., Harangozo 1993; Hoeke et al. 2013).

Wind waves are of great practical importance to coastal protection (e.g., Roelvink et al. 2009). Wave energy flux is a key driver of coastal erosion and contributes significantly to the evolution of shorelines, for example through modification of beach profiles due to sea level rise (Bruun 1962). Wind waves also play a role in flooding through overflowing, overtopping and breaching of natural barriers (e.g., dunes) or flood defences (e.g., dykes). Coastal flooding impacts are different in character in each case. Overflowing refers to when the water level (which includes wave setup) exceeds the height of the barrier. In the case of overtopping, when the crests of the waves exceed the barrier height, water with high momentum pours intermittently onto the coastal land. When breaching occurs, even greater flooding can take place, as the original barrier is no longer effective.

In spite of their importance, waves are often ignored in sea level studies, especially when those studies are not focused on extreme events. As waves propagate into shallow water, wave amplitudes increase until the waves become unstable and break (Dodet et al. 2019, in review). Breaking and wave dissipation raise water levels in the surf zone in a process known as wave setup (Fig. 6). The reduction in wave energy due to breaking leads

to a radiation stress gradient, with momentum transferred from waves to the water column (Longuet-Higgins and Stewart 1962; Bowen et al. 1968; Holman and Sallenger 1985; Dean and Walton 2009; Pugh and Woodworth 2014). Assuming steady-state conditions, the radiation stress gradient is balanced by higher water levels at the shore. Wave setup is proportional to the offshore significant wave height and can contribute to elevated water levels that are an appreciable fraction (20–30%) of the incident deep water significant wave height. The magnitude of setup can be estimated if one has either measured or modelled wave data and has knowledge of coastal bathymetry (e.g., Stockdon et al. 2006; Dietrich et al. 2009; Melet et al. 2016; Marsooli and Lin 2018; Pedreros et al. 2018). Spatial gradients in wave setup, due, for example, to variations in breaker height, can cause local circulations such as rip currents. Characteristic periods of wave setup are tens of the dominant incident wind-wave periods (O(1 min)). However, it is modulated on longer timescales through its dependence on the height, period and direction of incident waves and on the still water level (Idier et al. 2019, in review).

Wave setup is a particular concern for island shorelines that are otherwise protected from wave energy by coral reefs (Vetter et al. 2010; Becker et al. 2014; Hoeke et al. 2015; Buckley et al. 2018). At these locations, wave setup can be the largest single non-tidal contributor to extreme water levels (Merrifield et al. 2014).[2]

Because tide gauges are usually located in large protected harbours, where wave breaking is limited, wave setup in most cases will be negligible in tide gauge records, although notable exceptions can occur (e.g., Thompson and Hamon 1980; Aucan et al. 2012). In these cases, it can be appreciated that, although wave events and wave setup occur on the 'daily' timescale, wave setup will inevitably contribute to MSL variability on seasonal and even interannual timescales. Consequently, there is a possibility in some cases of contamination of existing long-term MSL records by variations in wave setup in the past, and the character of that contamination might change again if wave climate changes in the future (Melet et al. 2018, discussed in Aucan et al. 2019 and Melet et al. 2019). For example, in the Arctic, wave climate will depend on future sea ice conditions (Stopa et al. 2016). A further technical issue is that tide gauge measurements, whatever the technique employed, can be affected to some extent by waves (e.g., see discussion of wave effects on radar tide gauge data in Intergovernmental Oceanographic Commission, IOC 2016).

Before leaving waves, we can refer to a further process called 'swash' (Fig. 6). Wave swash is the oscillation in shoreline position due to wave propagation onto upper parts of the beach. It plays an important role in shaping the coastline through sediment transport, and in flooding through overtopping and breaching. Wave runup is defined as the combination of wave setup and swash, with setup being the mean component of runup averaged over some time window, and swash therefore having zero contribution to sea level over that window. On wave-exposed, open-coast beaches, wave runup can reach several metres during extreme events (Kennedy et al. 2016; Poate et al. 2016) and at times wave energy can cause significant modifications to the coast (e.g., Cox et al. 2018). Like setup, the importance of swash is site dependent, being determined by the height, period and direction of the incident waves. Therefore, it is modulated at low frequencies in a similar way to wave

[2] A distinction is usually made between low-frequency modulation of waves on the timescale of wave groups, which is sometimes called surf beat, and longer-term averages of the wave field associated with a steady setup component. Dynamically, setup is generally computed assuming that steady state, over a timescale in which acceleration terms are small compared to other terms in the momentum balance (say longer than about 15 min).

setup. However, unlike setup, it does not contribute to variability in what we refer to usually as 'sea level'.

5.2 River Runoff

A process with a similar potential contribution to coastal sea level measurement across a wide range of timescales is freshwater runoff from rivers (Durand et al. 2019, in review). The process is known to contribute to signals of the order of centimetres in sea level variability on daily timescales for some rivers in Europe, with plumes extending ~10 km from the river mouth (e.g., Laiz et al. 2014). Gómez-Enri et al. (2017) have suggested that such discharges of small rivers can be detected as sea surface height anomalies in coastal altimeter data. Runoff will undoubtedly be a much larger factor in large river deltas. For example, Wijeratne et al. (2008) pointed to the large (~1 m) seasonal cycle in MSL in the Ganges Delta, although it is not clear whether this is due to only runoff per se, or also to an associated thermosteric contribution (Fabien Durand, private communication; Neetu et al. 2012). Meade and Emery (1971) suggested a link between runoff and interannual variability in MSL at US tide gauges, a link which has been confirmed by recent research (Piecuch et al. 2018). The most extreme contribution from runoff is probably that associated with the Amazon River (e.g., Korosov et al. 2015), where the spreading of the river plume can be traced for distances larger than a 1000 km from its mouth. A climate model simulation by Jahfer et al. (2015) has shown that Amazon runoff can impact climate and sea level in a much broader sense, by contributing to the strength of the Atlantic Meridional Overturning Circulation (AMOC).

6 Seasonal Variability in Coastal Sea Level

The seasonal cycle is one of the most important non-tidal components of sea level records, especially in the mid- to high latitudes.[3] Seasonal variability in sea level is forced by a variety of mechanisms, including atmospheric pressure and winds, precipitation, river runoff, ice melting, ocean circulation changes and variations in steric height. The latter, driven by expansion/contraction of the water column above the seasonal thermocline in response to heat flux exchanges with the atmosphere, is the dominant contributor in most oceanic regions (Gill and Niller 1973).

The mean seasonal sea level cycle at the coast was investigated by Tsimplis and Woodworth (1994) using a data set of 1043 tide gauges distributed globally around the world coastlines. They reported high spatial variability in the annual and the semi-annual signals with annual amplitudes reaching several decimetres along some parts of the coast. However, coastal seasonal oscillations may significantly differ from those in the open ocean (Vinogradov and Ponte 2010). While in the deep ocean the annual cycle is driven by steric changes and the large-scale wind field (Chen et al. 2000; Vinogradov et al. 2008), near the coast other factors, such as local wind patterns, rivers or seasonal upwelling/downwelling, become dominant (Middleton and Cirano 1999; Middleton 2000). In general, annual amplitudes are larger along the coasts and over continental shelves due to the impact of

[3] The seasonal cycle of MSL also contains small long-period astronomical tidal contributions with periods of 6 months and 1 year (Pugh and Woodworth 2014).

these coastal processes. Seasonal changes in the atmospheric forcing also induce variability at these timescales in higher-frequency processes such as storm surges, which result in larger extremes of sea level during the winter season (Menéndez and Woodworth 2010; Merrifield et al. 2013; Marcos and Woodworth 2017). The same applies for offshore wave conditions as a result of the seasonality in storminess and thereby in the propagation of swell waves (e.g., Semedo et al. 2011). Seasonal changes in wave height, period and direction are more pronounced in extratropical regions, and highest in the Northern Hemisphere (Young 1999). As a result, wave setup also contributes to seasonal water level changes at the coast (Melet et al. 2016).

The major constituents of the ocean tide also display seasonality. For example, Pugh and Vassie (1976, 1992) demonstrated that the amplitude of the predominant M_2 constituent along North Sea coasts varies through the year by several per cent and is a maximum in summer. This variation is due to a well-developed thermocline in summer and a well-mixed water column during winter (Müller 2012; Gräwe et al. 2014). Similar variations have been observed in other shelf areas (e.g., Yellow Sea, Kang et al. 1995, and the Canadian Pacific, Foreman et al. 1995). As far as we know, such studies have not been made on a global basis. However, inspection of the Admiralty Tide Tables (UK Hydrographic Office, UKHO 2017) and other tidal databases shows evidence for similar seasonality in other shelf areas. One suspects that it is not so apparent at deep-ocean islands where tidal amplitudes anyway tend to be smaller than in continental shelf areas.

Despite the seasonal sea level cycle often being considered as a steady signal, many studies have reported significant temporal changes in seasonality. Interannual to multi-decadal variability has been related to changes in atmospheric pressure and wind fields (e.g., Plag and Tsimplis 1999, in the North and Baltic Seas; Marcos and Tsimplis 2007, in Southern Europe; Torres and Tsimplis 2012, in the Caribbean Sea) which, in turn, are linked to climate indices such as NAO. They have also been associated with variability in ocean currents, especially where these are strong (e.g., in the NW Pacific (Feng et al. 2015) or western Atlantic (Calafat et al. 2018)), or to changes in large-scale forcing patterns in steric height or sea surface temperature (SST) (Wahl et al. 2014). The study of Amiruddin et al. (2015) made use of both tide gauge and altimeter data from the South China Sea, finding significant differences between the coastal seasonal cycle and that of the nearby deeper ocean. Both types of data have also been applied to studies of the coastal seasonal cycle on a quasi-worldwide basis by Etcheverry et al. (2015), finding differences of ~2 cm between data types in the observed amplitudes of the annual cycle of MSL.

7 Interannual and Decadal Sea Level Variability

7.1 Importance of Climate Modes to Interannual Variability

Climate modes are large-scale patterns of coherent variability in meteorological or oceanographic parameters such as air pressure or SST, with the amplitude of the variability represented by a mode index. Since these parameters, and additional ones associated with them (e.g., winds), are known to be forcings of sea level variability (e.g., see Sect. 4 for discussion of wind forcing), it is unsurprising that large-scale patterns of variability in mean and extreme sea levels similar to the climate modes have also been observed (e.g., Menéndez and Woodworth 2010). Han et al. (2017a, b, 2018a, b) have already provided an overview

of ocean modes, with a focus on the Pacific and Indian Oceans. We comment below on the importance of such modes from the primary perspective of coastal sea level.

The modes have large impacts on coastal oceans by means of forcing by local winds associated with them and by remote influence from the ocean interior. For example, surface winds associated with the El Niño–Southern Oscillation (ENSO) and Indian Ocean Dipole (IOD), discussed below, induce eastward-propagating equatorial Kelvin waves; upon arriving at the eastern boundary, the energy subsequently propagates poleward as coastal trapped waves, affecting sea level in a long distance along the coastlines of the eastern Pacific (e.g., Enfield and Allen 1980) and eastern Indian Ocean, respectively.

ENSO is the best-known climate mode, consisting of a coupled atmospheric and oceanic oscillatory mode that originates in the tropical Pacific and acts on typical timescales of 5–7 years. ENSO 'warm events' are characterised by both a lowering of sea level air pressure and a weakening of the easterly trade winds over the eastern tropical Pacific, allowing an area of anomalously high SST to spread eastwards, accompanied by a shift in the main area of convection from Indonesia to the central Pacific (Rasmussen and Carpenter 1982). This reduces upwelling, deepens the thermocline and increases sea levels at the eastern boundary. In contrast, 'cold events' or 'La Niña' episodes are associated with anomalously low SST in the central and eastern Pacific and warmer surface waters to the western Pacific, which strengthens the easterly trade winds, increasing upwelling at the eastern margins. In both warm and cold events, sea level anomalies are transmitted polewards along the Pacific coast of the Americas in the form of coastal trapped Kelvin waves (Enfield and Allen 1980; Pugh and Woodworth 2014). Recently, Merrifield and Thompson (2018) have pointed to differences in ENSO climatology between the pre-1970 period, when ENSO variability was relatively low, and post-1970 when it was greater. The effects of ENSO are widespread, and ENSO influences have been identified in MSL variability along both the Pacific and Atlantic coastlines of the USA (Hamlington et al. 2015), while Marcos and Woodworth (2017) noted an ENSO influence on wintertime extreme sea levels along the US Atlantic coast.

In polar regions, annular climate modes dominate atmospheric variability, reflecting the meridional pressure contrast between a mid-latitude ring of high pressure and a polar low, which determines the strength of the westerlies in each hemisphere. In the Southern Hemisphere, Hall and Visbeck (2002) proposed the existence of a large-scale oceanic response to the Southern Annular Mode (SAM) or Antarctic Oscillation (AAO), describing how a positive state SAM index (associated with stronger eastward wind stress) would increase equatorward Ekman transport, coastal divergence and upwelling along the Antarctic coast, generating a simultaneous lowering of coastal sea levels and increased outcropping of isopycnals at the sea surface, and resulting in both a barotropic and a baroclinic response in circumpolar transport. Observational studies using sub-surface pressure (sea level corrected for the IB effect) from Southern Ocean coastal tide gauge and bottom pressure recorders have substantiated this, identifying a virtually instantaneous large-scale coherent and inverse sea level response to subseasonal variability of the SAM at coastal locations (Aoki 2002; Hughes et al. 2003; Meredith et al. 2004, Woodworth et al. 2006, Hibbert et al. 2010), with covariability having been shown to hold for interannual timescales in some studies (Hughes et al. 2003; Meredith et al. 2004, Hibbert et al. 2010).

The Northern Hemisphere counterpart to the SAM, the Northern Annular Mode (NAM) or Arctic Oscillation (AO), is characterised by centres of low air pressure over the Arctic and higher pressure over the North Pacific and central North Atlantic oceans. There is a close correspondence between this pattern and that of the NAO which is focused on the Icelandic Low and the Azores High, and it is usually agreed that the

NAO is a regional expression of the NAM (Thompson and Wallace 1998; Cohen and Barlow 2005).

Modelling studies of the Arctic Ocean suggest that coastal sea levels respond to periodic reversals of the ocean circulation (i.e. cyclonic or anticyclonic) (Proshutinsky and Johnson 1997; Proshutinsky et al. 2002; Dukhovsky et al. 2004), depending on the phase of the NAM (Newton et al. 2006; Proshutinsky et al. 2007). However, Häkkinen and Geiger (2000) reported the existence of two separate modes of sea surface height variability: one related to the NAM and a second associated with the NAO. Hughes and Stepanov (2004) used a barotropic model referenced to tide gauge observations, finding evidence of a highly coherent (but not dominant) Arctic Ocean sea level mode at interannual timescales that was associated with both the NAO and NAM. They concluded that variability of these atmospheric patterns caused changes in the eastward wind stress of atmospheric flows from the Atlantic, altering onshore Ekman flow and sea levels along the Arctic coast. These results are largely supported by observational studies (Dvorkin et al. 2000; Pavlov 2001, Proshutinsky et al. 2004; Richter et al. 2012; Calafat et al. 2013). Correlations between sea level and NAO/NAM decrease travelling east from the Norwegian Sea (Dvorkin et al. 2000; Calafat et al. 2013).

At lower latitudes, on the Eastern US coast, associations between the NAO and coastal sea levels have also been established (e.g., Andres et al. 2013), though it is unclear whether this arises from the dynamic effects of NAO-related variability on regional wind stress and air pressure (Andres et al. 2013; Ezer et al. 2013; Kenigson et al. 2018), or whether ocean heat anomalies associated with the NAO modulate the strength of the Atlantic Meridional Overturning Circulation, AMOC (Häkkinen 2000; McCarthy et al. 2015), or alternatively from some combination of the two (Goddard et al. 2015). Here, sea levels have been shown to exhibit a negative poleward gradient, with elevated sea levels in the vicinity of the subtropical gyre to the south of Cape Hatteras, and lower sea levels to the north in the colder waters of the sub-polar gyre. Variability in this sea level gradient has been strongly associated with heat exchange between the two gyres forcing changes in the AMOC, such that positive heat anomalies advected to the sub-polar gyre inhibit the AMOC (Bingham and Hughes 2009; Yin et al. 2009).

On the eastern boundary of the North Atlantic, a large-scale coherent sea level signal has been noted, which is highly correlated with the NAO at decadal timescales and which has been attributed to the association of the NAO with regional wind changes and to a lesser extent with air pressure (Wakelin et al. 2003; Miller and Douglas 2007; Calafat et al. 2012). The latter study noted that the region of coherent variability was largely confined to the continental shelf, postulating that along-shore winds force sea level anomalies that propagate polewards as coastal trapped waves (see below).

The Quasi-Biennial Oscillation (QBO) (Angell and Korshover 1964) describes a periodic reversal in the predominant direction (easterly or westerly) of the equatorial stratospheric winds that occurs approximately every 14 months. The phase of this is determined by upward fluxes of westerly and easterly momentum supplied by equatorially trapped Kelvin waves and Rossby-gravity waves, respectively (Lindzen and Holton 1968; Holton and Lindzen 1972), generating alternate wind regimes that gradually propagate downwards, dissipating at the tropopause. Unlike the climate modes discussed so far, the QBO is a stratospheric phenomenon, and, intuitively, a connection to sea level would be unexpected. However, Andrew et al. (2006) noted a statistically significant relationship between QBO index and sea level from altimetry in the tropical South Atlantic, but was unable to establish a dynamical explanation. Hibbert et al. (2010) identified an extratropical sea level response to the QBO along the coast of Antarctica, which was ascribed to modulation of

the westerlies by the poleward focusing of planetary wave activity during an easterly QBO phase.

There is also an important intraseasonal mode of tropical atmospheric variability called the Madden–Julian Oscillation (MJO) (Madden and Julian 1971). The MJO is characterised by the generation and eastward propagation of coupled atmospheric deep convection and precipitation anomalies on timescales of 30–100 days (Xie and Arkin 1997), but most commonly 40–50 days (Madden and Julian 1994). These eastward-propagating systems typically originate in the Indian Ocean and are discernible in observations of zonal wind and precipitation (Zhang 2005). Oliver and Thompson (2010) performed a global analysis of altimeter data, validated using tide gauge sea levels, and established three key regions of strong connection between sea level and the MJO, the most significant of which was found to be the equatorial region and eastern boundary of the Pacific. It was suggested that zonal winds induced sea level anomalies that propagate eastwards along the equator and then polewards in both hemispheres along the coast of the Americas in the form of coastal trapped waves. Along the coast of Sumatra, a similar mechanism was proposed, but in this case, the poleward-propagating waves were thought to be accompanied by westward-travelling Rossby waves. In contrast, sea level setup by MJO-related onshore winds was the underlying mechanism in the Gulf of Carpentaria. Matthews and Meredith (2004) identified a sea level response to the MJO on the Antarctic coast, which was attributed to the development of an extratropical atmospheric wave train.

Similar large-scale patterns to those of variability in coastal MSL associated with climate modes have also been observed in extreme sea levels (Menéndez and Woodworth 2010; Marcos et al. 2009; Talke et al. 2014; Marcos et al. 2015; Wahl and Chambers 2016). For example, a strong wintertime dependence of MSL and storm surge elevations on the NAO has been noted on the NW European shelf (Wakelin et al. 2003; Woodworth et al. 2007; Marcos and Woodworth 2017). Interannual changes in wind-wave height, period and direction are also influenced by climate modes (e.g., Semedo et al. 2011; Stopa and Cheung 2014 and references therein). Wave-driven processes in the coastal zone are therefore also directly dependent on large-scale teleconnection patterns such as ENSO, SAM and PDO (Pacific Decadal Oscillation), with remote responses of wave setup and runup through the propagation of swell across ocean basins (and, in turn, as noted above, wave setup can contribute to coastal sea level, Melet et al. 2018). Similarly, rates of coastal erosion will be affected by the variability in storm surges, MSL and wave direction and energy flux, and consequently will have a dependence on climate modes. Such an association between coastal erosion and ENSO has been observed on Pacific coasts (Barnard et al. 2015).

7.2 Decadal Sea Level Variability

Decadal variability can perhaps be claimed to be more important than interannual variability in some respects, owing to the longer periods being more comparable to the lengths of sea level records, and thereby being a determining factor in obtaining reliable secular sea level trends. Two of the main climate modes that exhibit energetic decadal timescale variability are the Pacific Decadal Oscillation (Mantua and Hare 2002) and the Indian Ocean Dipole (IOD) (Saji and Yamagata 2003). (In fact, the PDO also has an energetic interannual component. However, it has proportionally more decadal energy than ENSO modes.)

The PDO occurs in the same ocean areas as ENSO (primarily the Pacific), but on longer timescales, as reflected in Pacific SST north of 20°N. The IOD is a quasi-periodic oscillation of SST between the western and eastern tropical Indian Ocean, which impacts

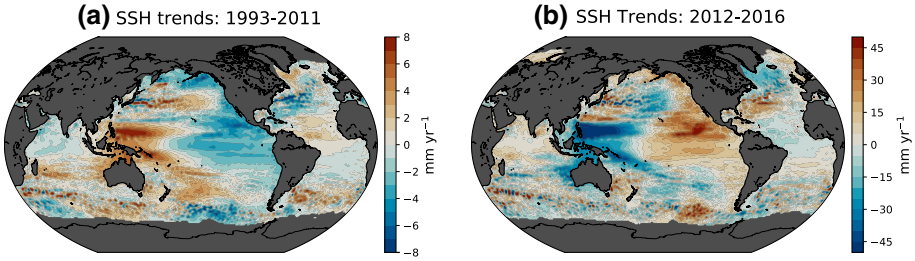

Fig. 7 Sea surface height (SSH) trends from **a** 1993 to 2011 and **b** from 2012 to 2016 based on Aviso gridded SSH data. These patterns in SSH trends are similar to those in sea surface temperatures, these two periods being times of decreasing and increasing PDO index, respectively. Adapted from Merrifield and Thompson (2018)

significantly on the regional monsoonal weather. Major IOD events occur less frequently than ENSO ones, but the two phenomena are clearly linked components of the climate system.

Although these two decadal indices are defined in terms of SST, they are also reflected in similar regional patterns of sea level change. For example, Merrifield and Thomson (2018) (see also Hamlington et al. 2016) pointed to a shift in PDO index and trade wind fields between 1993–2011 and 2012–2016 which manifests itself in patterns of sea level change of opposite sign in the two periods (Fig. 7). Reviews of Indian Ocean decadal variability, including discussion of the IOD and sea level, are given by Han et al. (2014, 2018a, b).

All of these decadal signals are regional, or even basin scale, in extent, rather than being particularly coastal. Nevertheless, the temperature and sea level variability associated with them can result in coastal impacts in, for example, coral bleaching or flooding of low-lying coral islands (e.g., Dunne et al. 2012).

Finally, one can mention that the nodal astronomical tide will contribute to variability in MSL. If this has a magnitude comparable to its equilibrium expectations, then it will be at the centimetre level or less at most locations (Woodworth 2012). Occasionally, larger nodal signals are reported in analyses of tide gauge data (e.g., Baart et al. 2012). However, these anomalous findings are mostly likely due to localised sea level variability (e.g., in river estuaries), or to genuine ocean variability with a similar period that is not adequately separable from the nodal tide in a short record.

8 Coastal Circulation Dynamics and Sea Level

The dynamics of the coastal ocean circulation are controlled by, amongst other things, bathymetry and the shape of the coastal boundaries. The dynamics introduces differences in sea level variability observed both along-shore and between the coast and deep ocean. These dynamics are discussed in detail by Hughes et al. (2019). However, for present purposes, we can point to three important aspects which are demonstrated in many studies: (1) the relative importance to sea level variability of atmospheric forcing, in particular wind stress, in shallow shelf seas, (2) the benefit of taking (1) into account when looking for longer-term trends in sea level variability, and (3) the sea level responses to forcing propagate along the shelf and slope, primarily cyclonically around an ocean basin (i.e. in the sense of Kelvin waves).

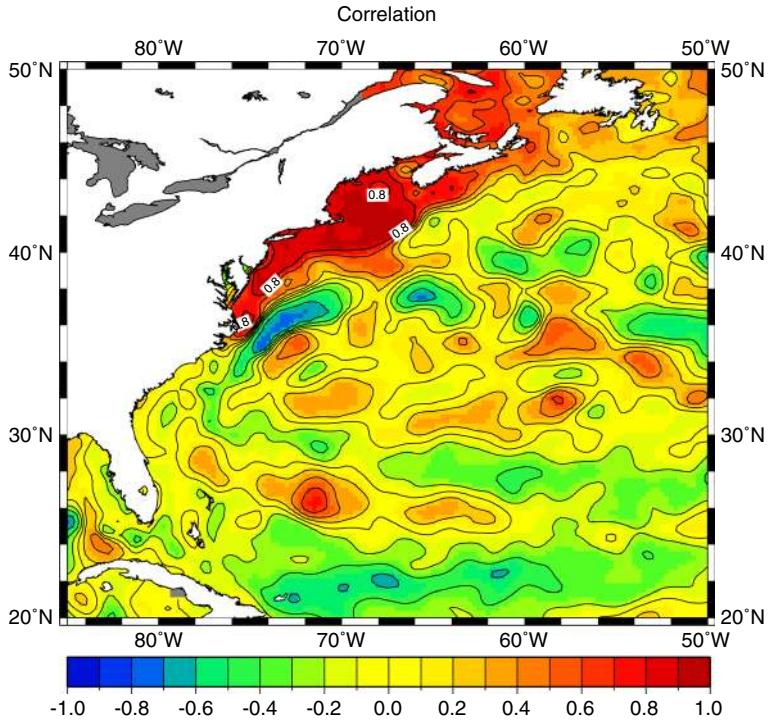

Fig. 8 Correlations of detrended annual mean values of sea level from altimeter data over 1993–2009 with those at a point on the shelf to the east of Cape Cod (42°N, 69°W). Sea level on the shelf can be seen to vary differently from that in the ocean. From Woodworth et al. (2014)

Dynamical processes along continental shelves have been investigated most intensively along the Atlantic coast of North America, where there is interesting dynamics related to the Gulf Stream, and high-quality tide gauge and meteorological data sets are available (e.g., Thompson and Mitchum 2014; Frederiske et al. 2017). The latter found a strong correlation between coastal sea level and decadal steric variability in the subpolar gyre which is probably caused by variability in the Labrador Sea that is propagated southward. They cite theory and modelling literature regarding coastal trapped waves as an explanation of the findings from their analysis of sea level measurements showing this propagation. The steric signal explains the majority of the observed decadal sea level variability. Much other research has focused on differences in variability north and south of Cape Hatteras and between shelf and deep ocean (Woodworth et al. 2014, 2017a; McCarthy et al. 2015), interannual variability north of the Cape being largely wind-driven over the shelf (Andres et al. 2013; Piecuch et al. 2016; Kenigson et al. 2018), while that to the south is controlled more by fluctuations in the Gulf Stream. As a result, coastal sea level variability, especially in the north, has little correspondence to that in the nearby deep ocean (Fig. 8). In addition, balances between the forces of bottom and lateral friction, which are larger where the flow is faster, and sea level gradient, result in along-shore tilts in sea level being smaller than in the deep ocean. In this situation, the sea level variations observed at the coast are said to be insulated from those in deeper ocean by the shelf (Fig. 9) (Higginson et al. 2015).

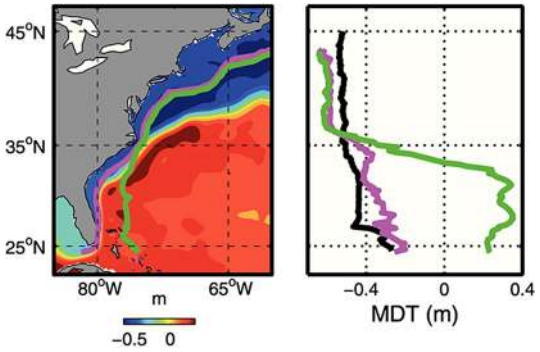

Fig. 9 (left) Mean dynamic topography (MDT) (in m) from the HYbrid Coordinate Ocean Model (HYCOM) data-assimilative ocean model. The magenta and green lines show the smoothed location of the 200 m and 2000 m isobaths, respectively. (right) MDT along the coastline (black) and along the 200 m (magenta) and 2000 m (green) isobaths, plotted against latitude. Note that the Gulf Stream signal in green is much attenuated on the shelf. From Higginson et al. (2015)

Links have been made between changes in the strength of the overturning circulation and sea level gradients on the US coast (Bingham and Hughes 2009; Yin et al. 2009; Yin and Goddard 2013). Consequently, the high rates of sea level rise ('accelerations') observed in recent years at stations in the Middle Atlantic Bight have been interpreted in terms of overturning changes (Sallenger et al. 2012; Boon 2012) with possible additional Greenland and Antarctic mass loss changes (Davis and Vinogradova 2017). Other links have been made between coastal sea level gradients, the strength of the Gulf Stream circulation and climate indices including the NAO (McCarthy et al. 2015) and the Atlantic Multidecadal Oscillation (AMO), an index defined by Atlantic sea surface temperatures (Kenigson and Han 2014). Most recently, Domingues et al. (2018) suggested two processes at work: warming of the Florida Current in the south, and air pressure changes in the north.

Sea level variability on the eastern boundary of the North Atlantic has been shown to be controlled largely by along-shore wind stress (Calafat et al. 2012). It is not known at present what the across-shelf spatial scale of such variability is, and so whether it can be considered 'coastal'. Nevertheless, one can suggest that it is due to a first-mode coastal trapped wave. Such a coastal trapped wave has the form of a Kelvin wave confined to the shelf, if the shelf width exceeds the barotropic radius of deformation at that location, and with the wind stress having a spatial scale exceeding the shelf width. There will be an along-shelf flow in the same sense across the whole shelf, with a node (zero) of elevation near the shelf break (Huthnance 1992). In the North Sea, Dangendorf et al. (2014) found that local atmospheric forcing mainly initiates MSL variability on timescales up to a few years; the IB effect being important in the northern North Sea, and wind stress in the shallower southern North Sea which is susceptible to storm surges. On decadal timescales, MSL variability was found to mainly reflect steric changes, which are largely forced remotely. They found evidence for a coherent signal extending between the Canary Islands and the Norwegian shelf, supporting the theory that along-shore wind forcing along the eastern boundary of the North Atlantic may cause coastal trapped waves that propagate thousands of kilometres along the continental slope. Similarly, Thompson et al. (2014) emphasised the need to account for atmospheric forcing and especially wind stress along North East Pacific coasts. They found that along-shore wind stress and local wind-stress curl are less important than (remote) equatorial forcing, the response to which propagates northwards.

Some general points can be made on the importance of along-shore winds based on the above literature. In the idealised context of uniform forcing and straight uniform shelf and slope, an along-shore wind tends to accelerate along-shore flow against bottom friction. The Coriolis force sets up cross-shelf transport which affects sea surface elevation at the coast relative to offshore (on the scale of the Rossby radius of deformation, or the shelf width if less). This sea surface slope balances the accelerating along-shore flow geostrophically, if bottom friction is relatively weak. Stronger friction tends to align the surface slope with the wind stress and limit the flow magnitude. Non-uniform or time-dependent forcing and non-uniform shelves result in propagating wave responses, so that the influence of the forcing extends over wave decay distances (greater for wide shelves and weak friction). Responses around very large islands may be considered in the same way. However, islands of much smaller scale than the forcing will experience an approximate averaging of the surrounding oceanic sea level.

Returning to the Pacific, the ENSO-related coastal sea levels along the American coast have already been referred to above. On the western side of the North Pacific, the Kuroshio Extension (KuE) provides the western boundary current of the subtropical gyre and is the Pacific counterpart of the Gulf Stream after separation at Cape Hatteras. As for the case of the Gulf Stream, interannual to decadal fluctuations of the KuE can have large impacts on coastal sea level variability.

Sasaki et al. (2014) have researched sea level variability along the coasts of Japan, primarily on decadal timescales. The first empirical orthogonal function (EOF) mode of sea level variability in the KuE region had previously been shown to describe well the meridional displacements of the KuE on decadal timescales (e.g., Taguchi et al. 2007). Sasaki et al. (2014) found that northward shifts of the KuE jet and the Kuroshio Current southeast of Japan are accompanied by higher sea levels at the coast. The decadal variability of the KuE latitude is mainly induced by westward-propagating, wind-forced Rossby waves from the eastern North Pacific (Qiu and Chen 2005; Yasuda and Sakurai 2006). These waves are concentrated along the KuE jet axis as jet-trapped Rossby waves. The resulting sea level changes along the Japan coast were found to be spatially variable, with large values along the south-eastern coast that are directly influenced by the jet-trapped Rossby waves, and also on the west coast, but small values north of the KuE jet. This is because any wind-induced Rossby waves will be trapped along the KuE axis (Sasaki et al. 2013). Hence, the area north of the KuE becomes a shadow zone which an incoming Rossby wave does not enter (Sasaki et al. 2014). Instead, a wind-forced coastal wave is one of the causes of interannual coastal sea level variability north of the KuE (e.g., Nakanowatari and Ohshima 2014). Kourafalou et al. (2015) described a case study, from the perspective of ocean forecasting, of an event in September 2011 that caused flooding in southern Japan. Sea level anomalies of ~30 cm were observed that resulted from the passage of coastal trapped waves induced by short-term fluctuations of the Kuroshio around 34°N, 140°E.

Sasaki et al. (2014) stress the importance of understanding the dynamical reasons for such variability in order to reliably predict future sea level changes. In a later modelling study of Japan sea level variability over 1906–2010, Sasaki et al. (2017) further pointed to the need to understand natural variability on decadal timescales for understanding future regional sea level change.

Another interesting feature is the bimodality of the Kuroshio path south of Japan. That changes between a straight path (along the south coast of Japan) and a large-meander path (away from the coast) on interannual to decadal timescales. This path variability induces sea level changes of about 10 cm along the south coast of Japan (Kawabe 1988; Usui et al. 2011). The Kuroshio transport, which is determined by the large-scale wind, is a key factor in

determining the Kuroshio path (e.g., Tsujino et al. 2013). Its transport in the East China Sea has been found to be highly correlated with the PDO (Andres et al. 2009). The variability of the Kuroshio transport also causes coastal sea level change in the upstream region, such as along the coasts of Taiwan (Chang and Oey 2011) and Philippines (e.g., Zhuang et al. 2013).

Elsewhere in the Pacific and Indian Oceans, there has long been evidence for wind-driven coastal trapped waves along Australian coasts, mostly on monthly timescales. These include the coastal trapped waves on the south coast forced by strong westerly winds and the wide shelf, on the west coast that propagate southwards, and on the east coast propagating north (White et al. 2014 and references therein).

One interesting dynamical aspect of near-coastal sea level (or sub-surface pressure, SSP) variability concerns coherence of variability in SSP on intraseasonal timescales (timescales less than a year and not including the regular seasonal cycle) over great distances along the shelf and slope around continental boundaries (Hughes and Meredith 2006). The existence of such coherence, investigated first using altimeter data, has since been verified with ocean models (Roussenov et al. 2008; Hughes et al. 2018, 2019) and demonstrates that 'coastal' (or at least 'shelf slope') variability need not always be 'short spatial scale'.

With regard to sea levels on island coasts, we can mention the important role of eddies in the dynamics of the global ocean circulation. Open-ocean eddies have been found to be responsible for decimetric signals in some sea level records from ocean islands. For example, Mitchum (1995) relates 90-day oscillations at Wake Island (western Pacific) to Rossby waves propagating westwards (possibly from eddies generated by flow impinging on Hawaii). As Wake Island is very small and at latitude $<20°$, it is expected to show the surface oscillations of the arriving Rossby waves. Modelled differences between coastal sea levels observed at islands and in the open ocean (Williams and Hughes 2013) show poor correlation for islands surrounded by ocean in which a large fraction of steric variability is at frequencies and wavelengths lacking baroclinic Rossby wave propagation. This is more likely at higher latitudes, so that coherence between island and open-ocean sea level decreases away from the Equator, until at yet higher latitudes the steric signal decreases and coherence increases once again.

Finally, on a similarly small spatial scale, one can refer to coastal bays and estuaries and their interaction with larger-scale dynamics that is sometimes reflected in sea level. For example, Feng and Li (2010) discussed the flushing of coastal bays in Louisiana due to the passage of cold fronts. This process takes place on timescales of less than 40 h and results in sea level changes of ~25 cm. On longer timescales, the strong winds and air pressure variations which are important to the coastal dynamics on shelves and the large-scale ocean circulation discussed above can result in particularly energetic (several decimetre) sub-tidal sea level variability in bays and estuaries. Examples for the American coast are discussed by Salas-Monreal and Valle-Levinson (2008) and Waterhouse and Valle-Levinson (2010).

9 Long-Term Changes in MSL

A major consequence of climate change is sea level rise resulting from changes in the density of sea water (steric effect) and from water mass transfer from land to the ocean from melting glaciers, ice sheets and groundwater storage changes (Church et al. 2013). Analysis of the first years of altimeter data suggested that MSL might be rising at a greater rate near to the coast than in the nearby deeper ocean (Holgate and Woodworth 2004) although such a difference was not considered significant by others (White et al. 2005; Prandi et al. 2009), and, as far as we are aware, there is at present no evidence for such differences.

As the depths of coastal waters increase, then many of the processes mentioned above will change:

- Tidal wavelengths will increase, and tidal patterns over the continental shelves will change. In fact, coastal tides are already known to be changing (e.g., Woodworth 2010; Haigh et al. 2019) for reasons that are not well understood. Sea level rise will result in further changes to the tides (e.g., Devlin et al. 2017; Idier et al. 2017; Pickering et al. 2017);
- Storm surge spatial gradients and magnitudes will reduce because of their dependence on 1/depth (Pugh and Woodworth 2014);
- Changes to tides and surges imply changes to extreme sea levels;
- Ocean waves break when entering water with depths ~2.6 times the wave amplitude (Dean and Walton 2009). As the MSL rises, waves with greater height and larger periods will impinge on coastal zones, with associated changes in wave setup and runup (Chini et al. 2010). This will cause amplified potential flooding impacts (Arns et al. 2017);
- Climate change may result in modifications to large-scale climate patterns (ENSO, NAO, etc.) and associated wind fields (and also heat content), resulting in regional changes in MSL and extreme sea level (Kirtman et al. 2013).

In addition to changes due to the depth of coastal waters, coastal sea level could also be affected by other changes in response to climate change including:

- Changes in regional patterns of atmospheric surface pressure and winds;
- Changes in ocean circulation (e.g., strengthening/weakening of coastal currents and of upwelling/downwelling);
- Changes in wind fields also imply further changes in wind waves and, therefore, in changes in wave setup, runup and overtopping.

Trends in surface winds have been observed over the last few decades, with notably a strengthening of the westerlies in the Southern Ocean and of the trade winds in the Pacific (e.g., Young et al. 2011; Swart and Fyfe 2012; Takahashi and Watanabe 2016). Climate change projections for the twenty-first century indicate significant changes in annual mean wave conditions over large ocean regions, notably with increased wave energy in the Southern Ocean that will impact remote regions through northward swell propagation (Hemer et al. 2013). Wave-driven contributions to water level at the coast could, therefore, exhibit trends in response to climate change over parts of the global ocean (Melet et al. 2018), which could lead to important coastal impacts. Long-term changes in wave direction may also induce changes in wave refraction and diffraction patterns, in along-shore current and associated sediment transport due to non-normal wave incidence. Together with changes in wave energy, they could result in altered patterns of beach erosion/accretion, and position and orientation of the shoreline.

All of these aspects of sea level variability are linked in various ways. In particular, trends observed in extreme sea levels in tide gauge records have been found to be related to trends in local MSL (see Sect. 4). Therefore, a gradual increase in MSL can thereby rapidly increase the frequency and severity of coastal flooding (Sweet and Park 2014). It has been estimated that 10 to 20 cm of sea level rise expected by 2050 will more than double the frequency of extreme events in the tropics (Vitousek et al. 2017). Extreme wave energy fluxes are projected to increase during this century implying potentially amplified impacts

on the coast (Mentaschi et al. 2017). The many interactions between the various processes mentioned above are discussed in greater detail by Idier et al. (2019).

10 Vertical Land Movements at the Coast

Vertical land motion contributes to relative sea level change observed by tide gauges at the coast, which can therefore differ from a change in sea level in the open ocean observed by altimetry. In other words, the ocean volume could remain unchanged, and yet sea level changes and coastal impacts could be observed due to vertical land motion only. As a matter of fact, the vertical position of the land surface at the coast (measured relative to the centre of the Earth) could be changing as much as the position of the sea surface itself, sometimes by a factor of ten or more. For instance, coastal subsidence in excess of a centimetre per year has been observed at Manila, Philippines (Raucoules et al. 2013), due to sub-surface anthropogenic activities and at Grand Isle, Louisiana (Törnqvist et al. 2008; Kolker et al. 2011), due to a combination of natural and anthropogenic processes, whereas coastal uplift up to a centimetre per year has been observed in Fennoscandia (Kierulf et al. 2014) or at Hudson Bay (Sella et al. 2007) due to ice mass unloading from the last deglaciation and glacial isostatic adjustment (GIA). What is more, ignoring vertical land motion, especially in active tectonic regions, can result in mistakes in attributing the reasons for sea level change and thereby in adoption of strategies for protecting populations and assets against coastal flooding (Ballu et al. 2011). Therefore, vertical land motion deserves as much attention as climate change in coastal sea level studies.

In fact, there are many phenomena that can cause vertical land motion, operating at different time and spatial scales (Fig. 2 and Table 1), resulting both from natural processes (e.g., GIA, tectonics and sediment compaction) and from anthropogenic activities (e.g., groundwater depletion, dam building or settling of landfill in urban areas) over a broad range of space and timescales. GIA is the most widely known phenomenon, operating globally at decadal to millennia timescales for which geodynamic models are available on a global basis (e.g., Peltier et al. 2015). This geological process includes deformational, gravitational and rotational effects due to the waxing and waning of the great ice sheets. It is essential to know the rheology of the Earth's interior and the histories of the ice sheets in order to predict accurately the viscoelastic response of the solid Earth and the resulting rates of vertical land movement (crustal displacement). There are important differences in such geodynamic modelling if the melting of land ice relates to the late Pleistocene ice sheets or to the present-day ice sheets, although the calculations are based on the same physics. For instance, the rheological behaviour of the Earth's interior can be approximated to that of an elastic body for short (decade to century) contemporary timescales of melting (Tamisiea and Mitrovica 2011; Riva et al. 2017; Spada 2017).

Water mass redistributions on the Earth's surface, and the associated loading of the solid Earth, can also result in significant vertical land motion. These include natural processes such as non-tidal atmospheric, oceanic and continental water mass loading variations, operating at interannual to decadal timescales with vertical displacements of the order of a mm/year (Santamaría-Gómez and Mémin 2015). To a lesser extent (at the level of 0.5 mm/year over multidecadal timescales), anthropogenic activities associated with water impoundment behind dams (Fiedler and Conrad 2010) and groundwater depletion (Veit and Conrad 2016) can also be important.

Earthquakes are instantaneous co-seismic vertical displacements of the Earth's surface. However, the earthquakes themselves are only one aspect of a set of tectonic processes within the earthquake deformation cycle. That cycle consists of steady interseismic motion that can last for years, decades or longer, punctuated by the instantaneous displacements during the earthquakes themselves. Following the earthquakes, there will be a postseismic relaxation during which deformation will occur lasting months to years before reverting to steady interseismic motion. For example, Ballu et al. (2011) reported a steady interseismic subsidence of the order of a cm/year at Torres Islands, Vanuatu, in between the magnitude Mw 7.8 earthquakes of 1997 and 2009. Those two earthquakes resulted in sudden vertical displacements of several hundreds of millimetres (subsidence of 500–1000 mm in 1997 and uplift of about 200 mm in 2009). These vertical displacements in land level thereby translated into abrupt coastal sea level changes in the opposite direction (sea level rise in the case of land subsidence and sea level fall in the case of land uplift). One may note that in this case study the interseismic vertical land motion (~ 1 cm/year) was three times larger than the rise of global MSL observed during the satellite altimetry era. Hence, it can be seen that such geological processes can play major roles in magnifying coastal risks from sea level change at such locations.

Prediction of the epochs and magnitudes of co-seismic and postseismic displacements are still beyond the present-day means of geophysical modelling. However, some progress has recently been accomplished regarding the interseismic motion. Smith-Konter et al. (2014) used a 3-D elastic/viscoelastic earthquake cycle model of the San Andreas Fault System, and identified in the sea level records along the California coastline the tectonic signals associated with the flexure of the elastic plate caused by bending moments at the ends of the locked faults. Unfortunately, such estimates of tectonic vertical land motion are not yet readily available for regions outside California.

Magma flow and pressure in active volcanoes, whether associated with tectonic plate boundaries or hot spots, can cause large inflation/deflation ground deformation events over days to months, and sometimes even longer periods. For example, at Socorro Island, part of a shield volcano located 200 km west of the Pacific coast of Mexico, Cazenave et al. (1999) observed a large post-eruptive 30 cm subsidence of the island during the 3 years following a submarine volcanic eruption in 1993.

In delta regions, land subsidence occurs naturally through sediment compaction when water is lost from interstitial spaces caused by the weight of overlying sediment or through rearrangement of sediment particles (Törnqvist et al. 2008). Observed rates of deltaic subsidence over the last few decades range from 3 to 100 mm/year. For instance, average subsidence rates of 4–6 mm/year have been reported for the Ganges–Brahmaputra Delta (Brown and Nicholls 2015) with much larger rates up to 10–20 mm/year in densely populated areas. This includes an estimated long-term contribution from sediment loading and sea level rise during the Holocene amounting to 1.1–1.7 mm/year, depending on the values for lithospheric thickness and Earth mantle viscosity considered (Karpytchev et al. 2018). These are all significant rates of vertical land movement when compared to the 3 mm/year rate of global MSL rise observed by satellite altimetry over the same time span. In highly populated delta areas, the extraction of groundwater, oil and gas that fill pore spaces can significantly exacerbate, and sometimes dominate, the rate of compaction and resulting subsidence (Kolker et al. 2011).

Locally, all contributions to sea level changes are important, whether arising from oceanic or vertical land motion processes. The factors controlling relative sea level differ from one coastline to another, and oceanic effects may not be the largest. In some coastal regions of the world, vertical land motion clearly dominates. In other areas, they might

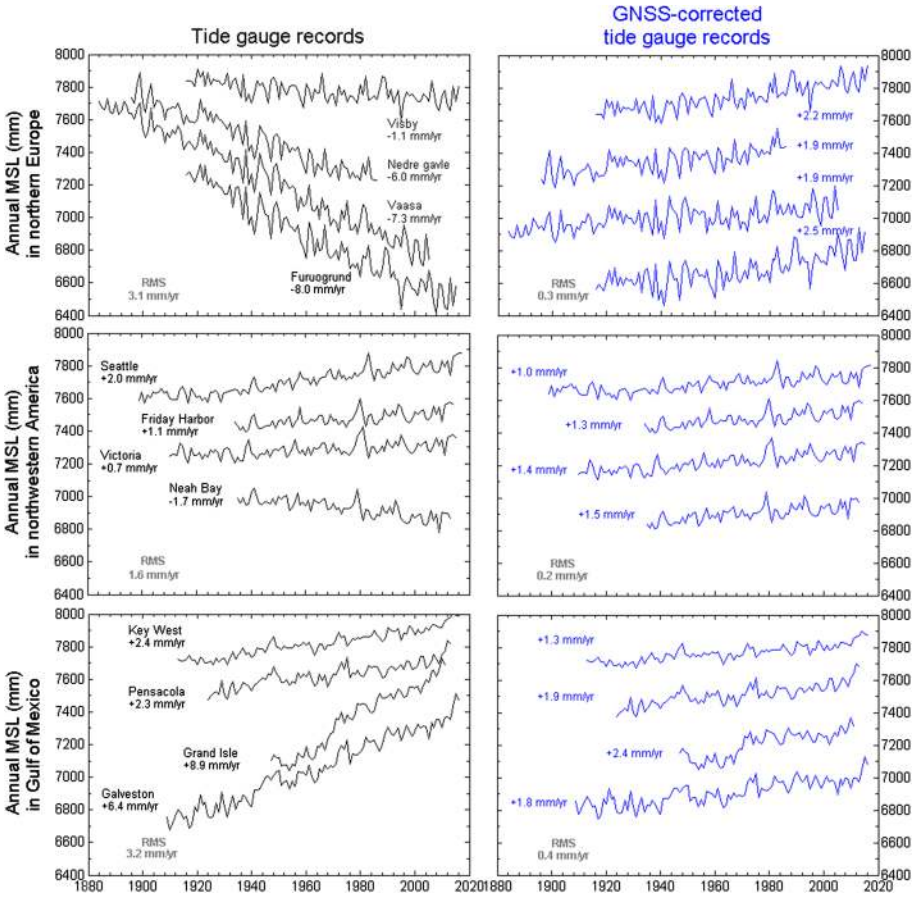

Fig. 10 Time series of annual MSL from (left) tide gauge records, and (right) GNSS-adjusted tide gauge records in (top) N Europe, (middle) NW America and (bottom) Gulf of Mexico. MSL data are from the Permanent Service for Mean Sea Level (PSMSL, https://psmsl.org), while GNSS information was acquired using the ULR6a solutions of the Système d'Observation du Niveau des Eaux Littorales (SONEL, http://www.sonel.org). The time series are displayed with arbitrary offsets for presentation purposes. Units mm. RMS indicates the root-mean-square of the trends shown in each panel

be of the same order of magnitude as oceanic (climate) factors (Wöppelmann and Marcos 2016). There is a clear need for measurements by modern geodetic techniques that provide accurate estimates of vertical land motion, which underlie the observed relative sea level changes, for application to sustainable management plans for the coast. This is why the new implementation plan of the international Global Sea Level Observing System (GLOSS) programme (see Marcos et al. 2019) calls for an important upgrade to its core network by requesting the installation of continuous Global Navigation Satellite System (GNSS) stations at tide gauges. GNSS will thereby measure the local vertical land movement of whatever origin. Figure 10 provides a demonstration of how trends of MSL measured by different tide gauges can be made more regionally consistent when GNSS information is employed to measure vertical land movements. The modern geodetic techniques are

also required to place the tide gauge data into the same geocentric reference frame as for the altimeter data as required for altimeter calibration studies (Mitchum 2000; IOC 2016).

11 Human Influences on Coastal Sea Level Variability

A full discussion of modifications in coastal sea level variability, which occur due to human intervention in coastal processes via coastal engineering, is outside the scope of this paper. However, several examples may be mentioned in order to demonstrate that there can indeed be such man-made impacts.

It is well known that the amplitudes and phases of tides in harbours and lagoons can be altered by engineering to their inlets, thereby altering the tidal prism. Similarly, both natural and anthropogenic changes in the sedimentation of coastal lagoons affect the tide (Araújo et al. 2008). Dredging in river estuaries will tend to lower low waters but leave high waters relatively unchanged, with a consequent increase in tidal range (Siefert 1982). Coastal engineering can affect the tides (de Boer et al. 2011), and schemes such as beach nourishment, which modify near-shore gradients, will modify wave setup and overtopping (Dean 1991). Similarly, a rise in MSL (which in itself could be said to be man-made) will modify the vertical profiles of some coastlines (Bruun 1962). MSL records exist which demonstrate the effect of human-induced sedimentation in coastal embayments (e.g., Manila), or the consequences of submergence due to ground water pumping (e.g., Bangkok, Shanghai), leading to anomalous local rates of relative sea level rise (see examples in Pugh and Woodworth 2014).

These examples demonstrate that the history of any changes to the area around a tide gauge station can be reflected in its record, as can relocations of recording within a large harbour, or changes in tide gauge technology.

12 Conclusions

We have shown that there are many processes which result in coastal sea level variability, operating on timescales from seconds to centuries and on spatial scales from local to global. Many of the processes (summarised in Table 1) are understood well (in principle at least), such as tides and surges, although some remain relatively little researched and underrepresented in sea level studies. In fact, there are others that have not been included here as they are not particularly coastal in character. Compendiums such as Pugh and Woodworth (2014) and Cazenave and Stammer (2017) provide more information on some of them, while several are discussed in greater detail in other papers in this volume. The scientific aim must be to be able to understand and model as many of these processes as possible.

We have also shown that each process will depend on the others to some extent due to the associated changes in water depth. It has also been shown that it is mistake to think that coastal sea level variability always has a ‘local’ forcing (although it often does), given that there are also for instance processes that result in signals trapped by and propagating along the continental shelves.

Some questions for consideration in future research are:

- How well can ocean models of various kinds reproduce the time series of sea level variability observed at the coast by tide gauges and offshore by altimetry (i.e. understanding the differences akin to those shown in Fig. 1)? Models will inevitably perform well for some regions and timescales, but less well for others (e.g., Chepurin et al. 2014; Becker et al. 2016; Meyssignac et al. 2017). In particular, models that are capable of reproducing coastal sea level variability observed to date will provide confidence in projecting future coastal sea level change (Ponte et al. 2019).
- Concerning our knowledge of tides at the coast, users of satellite altimetry in the deep ocean have grown accustomed to having reliable tide models that account for that dominant component of variability in their data. However, when altimetry is applied to the near-coastal zones, the existing models are less reliable and must be developed to greater complexity with many additional constituents. Deep-water versus shallow-water spectra (Fig. 3) readily convey the challenges of modelling coastal tides. In addition, a better determination and understanding is required of secular and other low-frequency changes in coastal tides that have been observed (this question relates to the need for 'data archaeology' mentioned below).
- With regard to waves, how much are historical MSL records contaminated by wave setup and can any contributions be modelled efficiently and so removed from the records? This question applies especially to composite records obtained from gauges at different locations within a bay or port. Should there be a comprehensive global coastal wave monitoring network to collect the data needed to assess the setup contribution to MSL? How will the wave setup contribution change in the future if wave climate changes?
- Similarly, how much have historical MSL records been contaminated by contributions from river runoff, and therefore misrepresent open-ocean conditions?
- There are several important questions in geodesy. How well can models of the solid Earth predict the motion (primarily vertical) of geodetic benchmarks at the coast over decadal to century timescales, specifically at tide gauges? Also, can the terrestrial reference frame be implemented in an accurate and stable manner in order to predict accurately the positions and motions of geodetic stations? Geophysical modelling and space geodesy observations have suggested that we should target vertical land motion predictability at the level of 0.1 mm/year over decadal to century timescales (Blewitt et al. 2010).
- In climate research, what mechanisms have been responsible for past changes in extreme levels (other than changes in MSL) and how might forcings and extremes change in the future? In particular, how will the extremely damaging storm surges associated with tropical cyclones change?
- In coastal modelling, because atmospheric forcing (and in particular wind stress) is relatively important in shallow shelf seas, there are challenges (1) to remove its shorter-term effects on coastal sea levels when estimating longer-term trends, and (2) to separate its longer-term effect from open-ocean sea level trends as drivers of coastal sea level change. Additionally, (3) as discussed in Sect. 8, because responses to forcing propagate along the shelf and slope, with forms and speed dependent on the shelf and slope topography, there is a need for models to be developed with sufficient resolution and 'upstream' extent over the distance in which the propagating signals decay. An additional challenge relates to modelling in greater detail the sea level variability around islands (including any surrounding shelves) located at different latitudes and with different sizes (larger and smaller than the baroclinic deformation radius) to understand where models and measurements differ.

Progress cannot be made with these and many other questions to do with sea level variability without access to the best, and most complete, observational and modelling data sets, as discussed further by Ponte et al. (2019). One may note:

- It is essential that the global network of tide gauges and other essential in situ data sets be completed and analysed in combination with satellite altimeter data sets (Roemmich et al. 2017). The global tide gauge network is currently challenged with maintaining many existing stations and installing new ones where required. Where appropriate, GNSS-reflection tide gauges may be more suitable than conventional techniques (Larson et al. 2017). In addition, there is a need for continuous monitoring of vertical land motion at tide gauges, requiring the installation of permanent GNSS stations at as many tide gauges as possible, and as near as possible to the tide gauges, and the undertaking of regular levelling campaigns between the tide gauge benchmarks and GNSS benchmarks (Woodworth et al. 2017b). See also discussion of this topic in Marcos et al. (2019) and Ponte et al. (2019).
- It is important also to extend the historical coastal sea level data set via a programme in 'data archaeology' (Bradshaw et al. 2015) and the use of 'proxy' (geological) data sets (e.g., Barlow et al. 2014).
- High-frequency (timescales ~ 1 h or less) sea level variability due to seiches, meteotsunamis and other high-frequency processes are frequently under-represented in sea level studies (Vilibić and Šepić 2017), and yet contribute to the extreme sea levels which are of great research interest and importance to coastal dwellers. In particular, an important objective should be to derive via barotropic modelling a global data set of seiche climatology.
- Similarly, it is highly desirable that barotropic tide-surge modelling, presently providing typically hourly values of modelled sea level on a global grid back to the mid-twentieth century, be extended back to the mid-nineteenth century using newly available reanalysis wind fields (Compo et al. 2011). Such model data sets would have many applications in understanding sea level variability.
- Access to new sets of coastal altimetry data, uncontaminated by reflections from the altimeter footprint over land and with improved geophysical corrections, should illuminate to a greater extent the reasons for differences between coastal and ocean sea level variability (Vignudelli et al. 2011; Cipollini et al. 2012, 2017; Birol et al. 2017). However, in our opinion, these data sets will never be a substitute for tide gauges in the coastal zone, given their temporal resolution and accuracy. The continuity of both in situ and space-based instrumentation is essential for a proper monitoring and understanding changes in sea level. The several techniques in combination will thereby enable us to understand as well as possible the evolution of coastal zones (Cazenave et al. 2017).

Acknowledgements We are grateful to Déborah Idier and Chris Piecuch for helpful comments. This work was supported partly by Natural Environment Research Council National Capability funding (for Woodworth, Hibbert and Huthnance) and by a research grant from CNPq (for Cirano). The paper arose from the Workshop on 'Understanding the Relationship between Coastal Sea Level and Large-Scale Ocean Circulation' held at the International Space Science Institute (ISSI), Bern, Switzerland, on 5–9 March 2018.

References

Airy GB (1878) On the tides at Malta. Philos Trans R Soc 169:123–138. https://doi.org/10.1098/rstl.1878.0006

Amiruddin AM, Haigh ID, Tsimplis MN, Calafat FM, Dangendorf S (2015) The seasonal cycle and variability of sea level in the South China Sea. J Geophys Res Oceans 120:5490–5513. https://doi.org/10.1002/2015JC010923

Andres M, Park J-H, Wimbush M, Zhu X, Nakamura Kim K, Chang K-I (2009) Manifestation of the Pacific decadal oscillation in the Kuroshio. Geophys Res Lett 36:L16602. https://doi.org/10.1029/2009GL039216

Andres M, Gawarkiewicz GG, Toole JM (2013) Interannual sea level variability in the western North Atlantic: regional forcing and remote response. Geophys Res Lett 40:5915–5919. https://doi.org/10.1002/2013GL058013

Andrew JAM, Leach HL, Woodworth PL (2006) The relationships between tropical Atlantic sea level variability and major climate indices. Ocean Dynam 56:452–463. https://doi.org/10.1007/s10236-006-0068-z

Angell JK, Korshover J (1964) Quasi-biennial variations in temperature, total ozone and tropopause height. J Atmos Sci 21:479–492. https://doi.org/10.1175/1520-0469(1964)021<0479:QBVITT>2.0.CO;2

Aoki S (2002) Coherent sea level response to the Antarctic Oscillation. Geophys Res Lett 29:11-1–11-4. https://doi.org/10.1029/2002gl015733

Araújo IB, Dias JM, Pugh DT (2008) Model simulations of tidal changes in a coastal lagoon, the Ria de Aveiro (Portugal). Cont Shelf Res 28:1010–1025. https://doi.org/10.1016/j.csr.2008.02.001

Ardhuin F, Chapron B, Collard F (2009) Observation of swell dissipation across oceans. Geophys Res Lett 36:L06607. https://doi.org/10.1029/2008GL037030

Arns A, Dangendorf S, Jensen J, Talke S, Bender J, Pattiaratchi C (2017) Sea level rise induced amplification of coastal protection design heights. Sci Rep 7:40171. https://doi.org/10.1038/srep40171

Aucan J, Hoeke R, Merrifield MA (2012) Wave-driven sea level anomalies at the Midway tide gauge as an index of North Pacific storminess over the past 60 years. Geophys Res Lett 39:L17603. https://doi.org/10.1029/2012GL052993

Aucan J, Hoeke RK, Storlazzi CD, Stopa J, Wandres M, Lowe R (2019) Waves do not contribute to global sea-level rise. Nat Clim Change 9:2. https://doi.org/10.1038/s41558-018-0377-5

Baart F, van Gelder PHAJM, de Ronde J, van Koningsveld M, Wouters B (2012) The effect of the 18.6-year lunar nodal cycle on regional sea-level rise estimates. J Coast Res 28:511–516. https://doi.org/10.2112/JCOASTRES-D-11-00169.1

Ballu V, Bouin MN, Siméoni P, Crawford WC, Calmant S, Boré JM, Kanas T, Pelletier B (2011) Comparing the role of absolute sea-level rise and vertical tectonic motions in coastal flooding, Torres Islands (Vanuatu). Proc Natl Acad Sci USA 108:13019–13022. https://doi.org/10.1073/pnas.1102842108

Barlow NLM, Long AJ, Saher MH, Gehrels WR, Garnett MH, Scaife RG (2014) Salt-marsh reconstructions of relative sea-level change in the North Atlantic during the last 2000 years. Quat Sci Rev 99:1–16. https://doi.org/10.1016/j.quascirev.2014.06.008

Barnard PL et al (2015) Coastal vulnerability across the Pacific dominated by El Niño/Southern Oscillation. Nat Geosci 8:801–808. https://doi.org/10.1038/ngeo2539

Becker JM, Merrifield MA, Ford M (2014) Water level effects on breaking wave setup for Pacific Island fringing reefs. J Geophys Res Oceans 119:914–932. https://doi.org/10.1002/2013JC009373

Becker M, Karpytchev M, Marcos M, Jevrejeva S, Lennartz-Sassinek S (2016) Do climate models reproduce complexity of observed sea level changes? Geophys Res Lett 43:5176–5184. https://doi.org/10.1002/2016GL068971

Bingham RJ, Hughes CW (2009) Signature of the Atlantic meridional overturning circulation in sea level along the east coast of North America. Geophys Res Lett 36:L02603. https://doi.org/10.1029/2008GL036215

Birol F, Fuller N, Lyard F, Cancet M, Niño F, Delebecque C, Fleury S, Toublanc F, Melet A, Saraceno M, Léger F (2017) Coastal applications from nadir altimetry: example of the X-TRACK regional products. Adv Space Res 59:936–953. https://doi.org/10.1016/j.asr.2016.11.005

Blewitt G, Altamimi Z, Davis J, Gross R, Kuo C-Y, Lemoine FG, Moore AW, Neilan RE, Plag H-P, Rothacher M, Shum CK, Sideris MG, Schöne T, Tregoning P, Zerbini S (2010) Geodetic observations and global reference frame contributions to understanding sea-level rise and variability. In: Church JA, Woodworth PL, Aarup T, Wilson WS (eds) Understanding sea-level rise and variability. Chapter 9. Wiley, London, pp 256–284

Boon JD (2012) Evidence of sea level acceleration at U.S. and Canadian tide stations, Atlantic coast, North America. J Coast Res 28:1437–1445. https://doi.org/10.2112/JCOASTRES-D-12-00102.1

Bowen AJ, Inman DL, Simmons VP (1968) Wave 'set-down' and set-up. J Geophys Res 73:2569–2577. https://doi.org/10.1029/JB073i008p02569

Bradshaw E, Rickards L, Aarup T (2015) Sea level data archaeology and the Global Sea Level Observing System (GLOSS). GeoResJ 6:9–16. https://doi.org/10.1016/j.grj.2015.02.005

Brown S, Nicholls RJ (2015) Subsidence and human influences in mega deltas: the case of the Ganges–Brahmaputra–Meghna. Sci Total Environ 527–528:362–374. https://doi.org/10.1016/j.scitotenv.2015.04.124

Bruun P (1962) Sea-level rise as a cause of shore erosion. J Waterways Harbors Div 88:117–130

Buckley ML, Lowe RJ, Hansen JE, van Dongeren AR, Storlazzi CD (2018) Mechanisms of wave-driven water level variability on reef-fringed coastlines. J Geophys Res Oceans 123:3811–3831. https://doi.org/10.1029/2018JC013933

Calafat FM, Chambers DP, Tsimplis MN (2012) Mechanisms of decadal sea level variability in the eastern North Atlantic and the Mediterranean Sea. J Geophys Res 117:C09022. https://doi.org/10.1029/2012JC008285

Calafat FM, Chambers DP, Tsimplis MN (2013) Inter-annual to decadal sea-level variability in the coastal zones of the Norwegian and Siberian Seas: the role of atmospheric forcing. J Geophys Res Oceans 118:1287–1301. https://doi.org/10.1002/jgrc.20106

Calafat FM, Wahl T, Lindsten F, Williams J, Frajka-Williams E (2018) Coherent modulation of the sea-level annual cycle in the United States by Atlantic Rossby waves. Nat Commun 9:2571. https://doi.org/10.1038/s41467-018-04898-y

Carrère L, Lyard F (2003) Modeling the barotropic response of the global ocean to atmospheric wind and pressure forcing—comparisons with observations. Geophys Res Lett 30:1275. https://doi.org/10.1029/2002GL016473

Cazenave A, Stammer D (eds) (2017) Satellite altimetry over oceans and land surfaces. CRC Taylor and Francis, Boca Raton, p 644

Cazenave A, Dominh F, Ponchaut F, Soudarin L, Cretaux JF, Le Provost C (1999) Sea level changes from Topex-Poseidon altimetry and tide gauges, and vertical crustal motions from DORIS. Geophys Res Lett 26:2077–2080. https://doi.org/10.1029/1999GL900472

Cazenave A, Le Cozannet G, Benveniste J, Woodworth P (2017) Monitoring the change of coastal zones from space. Eos, Transactions of the American Geophysical Union, 98. Published on 02 Nov 2017. https://eos.org/opinions/monitoring-coastal-zone-changes-from-space

Chang Y-L, Oey L (2011) Interannual and seasonal variations of Kuroshio transport east of Taiwan inferred from tide-gauge data. Geophys Res Lett 38:L08603. https://doi.org/10.1029/2011GL047062

Chen JL, Shum CK, Wilson CR, Chambers DP, Tapley BD (2000) Seasonal sea level change from TOPEX/Poseidon observation and thermal contribution. J Geodesy 73:638–647. https://doi.org/10.1007/s001900050

Chepurin GA, Carton JA, Leuliette E (2014) Sea level in ocean reanalyses and tide gauges. J Geophys Res Oceans 119:147–155. https://doi.org/10.1002/2013JC009365

Chini N, Stansby P, Leake J, Wolf J, Roberts-Jones J, Lowe J (2010) The impact of sea level rise and climate change on inshore wave climate: a case study for East Anglia (UK). Coast Eng 57:973–984. https://doi.org/10.1016/j.coastaleng.2010.05.009

Church JA, Clark PU, Cazenave A, Gregory JM, Jevrejeva S, Levermann A, Merrifield MA, Milne GA, Nerem RS, Nunn PD, Payne AJ, Pfeffer WT, Stammer D, Unnikrishnan AS (2013) Sea level change. In: Stocker TF, Qin D, Plattner G-K, Tignor M, Allen SK, Boschung J, Nauels A, Xia Y, Bex V, Midgley PM (eds) Climate change 2013: the physical science basis. Contribution of working group I to the fifth assessment report of the intergovernmental panel on climate change. Cambridge University Press, Cambridge

Cipollini P, Calafat FM, Jevrejeva S, Melet A, Prandi P (2017) Monitoring sea level in the coastal zone with satellite altimetry and tide gauges. Surv Geophys 38:33–57. https://doi.org/10.1007/s10712-016-9392-0

Cohen J, Barlow M (2005) The NAO, the AO and global warming: how closely related? J Clim 18:4498–4513. https://doi.org/10.1175/JCLI3530.1

Compo GP, Whitaker JS, Sardeshmukh PD, Matsui N, Allan RJ, Yin X, Gleason BE, Vose RS, Rutledge G, Bessemoulin P, Brönnimann S, Brunet M, Crouthamel RI, Grant AN, Groisman PY, Jones PD, Kruk M, Kruger AC, Marshall GJ, Maugeri M, Mok HY, Nordli Ø, Ross TF, Trigo RM, Wang XL, Woodruff SD, Worley SJ (2011) The twentieth century reanalysis project. Q J R Meteorol Soc 137:1–28. https://doi.org/10.1002/qj.776

Cook KH, Vizy EK (2010) Hydrodynamics of the Caribbean low-level jet and its relationship to precipitation. J Clim 23:1477–1494. https://doi.org/10.1175/2009JCLI3210.1

Cox R, Jahn KL, Watkins OG, Cox P (2018) Extraordinary boulder transport by storm waves (west of Ireland, winter 2013–2014), and criteria for analysing coastal boulder deposits. Earth Sci Rev 177:623–636. https://doi.org/10.1016/j.earscirev.2017.12.014

Dangendorf S, Calafat FM, Arns A, Wahl T, Haigh ID, Jensen J (2014) Mean sea level variability in the North Sea: processes and implications. J Geophys Res Oceans 119:6820–6841. https://doi.org/10.1002/2014JC009901

Daussy P (1831) Mémoire sur les Marées des côtes de France. Connaissance des Tems […] pour l'année 1834. Bureau des Longitudes, Paris, pp 74–87

Davis JL, Vinogradova NT (2017) Causes of accelerating sea level on the East Coast of North America. Geophys Res Lett 44:5133–5141. https://doi.org/10.1002/2017GL072845

de Boer WP, Roos PC, Hulscher SJMH, Stolk A (2011) Impact of mega-scale sand extraction on tidal dynamics in semi-enclosed basins. An idealized model study with application to the Southern North Sea. Coast Eng 58:678–689. https://doi.org/10.1016/j.coastaleng.2011.03.005

Dean RG (1991) Equilibrium beach profiles: characteristics and applications. J Coast Res 7: 53–84. https://www.jstor.org/stable/4297805

Dean RG, Walton TL (2009) Wave setup. Chapter 1 in, Handbook of coastal and ocean engineering. World Scientific Publishing Co. Ltd. http://www.worldscibooks.com/engineering/6914.html

Defant A (1961) Physical oceanography. Pergamon Press, London

Devlin AT, Jay DA, Talke SA, Zaron ED, Pan J, Lin H (2017) Coupling of sea level and tidal range changes, with implications for future water levels. Sci Rep 7:17021. https://doi.org/10.1038/s41598-017-17056-z

Dietrich JC, Bunya S, Westerink JJ, Ebersole BA, Smith JM, Atkinson JH, Jensen R, Resio DT, Luettich RA, Dawson C, Cardone VJ, Cox AT, Powell MD, Westerink HJ, Roberts HJ (2009) A high-resolution coupled riverine flow, tide, wind, wind wave, and storm surge model for Southern Louisiana and Mississippi. Part II: synoptic description and analysis of Hurricanes Katrina and Rita. Mon Weather Rev 138:378–404. https://doi.org/10.1175/2009MWR2907.1

Dodet G, Melet A, Ardhuin F, Bertin X, Idier D, Almar R (2019) The contribution of wind generated waves to coastal sea level changes. Surv Geophys (in review)

Domingues R, Goni G, Baringer M, Volkov D (2018) What caused the accelerated sea level changes along the United States East Coast during 2010–2015? Geophys Res Lett 45:13367–13376. https://doi.org/10.1029/2018GL081183

Dukhovsky DS, Johnson MA, Proshutinsky A (2004) Arctic decadal variability: an auto-oscillatory system of heat and fresh water exchange. Geophys Res Lett 31:L03302. https://doi.org/10.1029/2003GL019023

Dunne RP, Barbosa SM, Woodworth PL (2012) Contemporary sea level in the Chagos Archipelago, central Indian Ocean. Glob Planet Change 82–83:25–37. https://doi.org/10.1016/j.gloplacha.2011.11.009

Durand F, Piecuch C, Cirano M, Becker M, Papa F (2019) Runoff impact on coastal sea level. Surv Geophys (in review)

Dvorkin EN, Kochanov SY, Smirnov NP (2000) The North Atlantic Oscillation and long-term changes in the level of the Arctic Ocean. Russ Meteorol Hydrol 3:59–64

Enfield DB, Allen JS (1980) On the structure and dynamics of monthly mean sea level anomalies along the Pacific coast of North and South America. J Phys Oceanogr 10:557–578. https://doi.org/10.1175/1520-0485(1980)010<0557:OTSADO>2.0.CO;2

Etcheverry LAR, Saraceno M, Piola AR, Valladeau G, Möller OO (2015) A comparison of the annual cycle of sea level in coastal areas from gridded satellite altimetry and tide gauges. Cont Shelf Res 92:87–97. https://doi.org/10.1016/j.csr.2014.10.006

Ezer T, Atkinson LP, Corlett WB, Blanco JL (2013) Gulf stream's induced sea level rise and variability along the U.S. mid-Atlantic coast. J Geophys Res Oceans 118(2):685–697. https://doi.org/10.1002/jgrc.20091

Feng Z, Li C (2010) Cold-front-induced flushing of the Louisiana Bays. J Mar Syst 82:252–264. https://doi.org/10.1016/j.jmarsys.2010.05.015

Feng X, Tsimplis MN, Marcos M, Calafat FM, Zheng J, Jorda G, Cipollini P (2015) Spatial and temporal variations of the seasonal sea level cycle in the northwest Pacific. J Geophys Res Oceans 120:7091–7112. https://doi.org/10.1002/2015JC011154

FES2014 (2018) Description of the FES2014 ocean tide model, obtained from https://www.aviso.altimetry.fr/en/data/products/auxiliary-products/global-tide-fes/description-fes2014.html. Downloaded Jan 2018

Fiedler JW, Conrad CP (2010) Spatial variability of sea level rise due to water impoundment behind dams. Geophys Res Lett 37:L12603. https://doi.org/10.1029/2010GL043462

Flather RA (2000) Existing operational oceanography. Coast Eng 41:13–40. https://doi.org/10.1016/S0378-3839(00)00025-9

Forel F-A (1876) Note sur un limnimètre enregistreur établi á Morges (Lac Léman) pour étudier les seiches. Annales de Chimie et de Physique (5th series) 9:90–92

Foreman MGG, Walters RA, Henry RF, Keller CP, Dolling AG (1995) A tidal model for eastern Juan de Fuca Strait and the southern Strait of Georgia. J Geophys Res 100:721–740. https://doi.org/10.1029/94JC02721

Frederikse T, Simon K, Katsman CA, Riva R (2017) The sea-level budget along the Northwest Atlantic coast: gIA, mass changes, and large-scale ocean dynamics. J Geophys Res Oceans 122:5486–5501. https://doi.org/10.1002/2017JC012699

Gill AE (1982) Atmosphere–ocean dynamics. Academic Press, New York, p 662

Gill AE, Niller PP (1973) The theory of the seasonal variability in the ocean. Deep Sea Res Oceanogr Abstr 20(2):141–177. https://doi.org/10.1016/0011-7471(73)90049-1

Gille ST, Llewellyn Smith SG, Statom NM (2005) Global observations of the land breeze. Geophys Res Lett 32:L05605. https://doi.org/10.1029/2004GL022139

Goddard PB, Yin J, Griffies SM, Zhang S (2015) An extreme event of sea-level rise along the Northeast coast of North America in 2009–2010. Nat Commun 6:6346. https://doi.org/10.1038/ncomms7346

Gómez-Enri J, Vignudelli S, Cipollini P, Coca J, González CJ (2017) Validation of CryoSat-2 SIRAL sea level data in the eastern continental shelf of the Gulf of Cadiz (Spain). Adv Space Res. https://doi.org/10.1016/j.asr.2017.10.042 (in press)

Gönnert G, Dube SK, Murty T, Siefert W (2001) Global storm surges: theory, observations and applications. Die Küste Volume 63. http://www.kfki.de

Gräwe U, Burchard H, Müller M, Schuttelaars HM (2014) Seasonal variability in M2 and M4 tidal constituents and its implications for the coastal residual sediment transport. Geophys Res Lett 41:5563–5570. https://doi.org/10.1002/2014GL060517

Green JAM, Huber M, Waltham D, Buzan J, Wells M (2017) Explicitly modelled deep-time tidal dissipation and its implication for Lunar history. Earth Planet Sci Lett 461:46–53. https://doi.org/10.1016/j.epsl.2016.12.038

Gregory J, Hughes C, Stammer D, Griffies S, Idier D, Fukumori I, Ponte R (2019) Concepts and terminology for sea level: mean, variability and change, both local and global. Surv Geophys. https://doi.org/10.1007/s10712-019-09525-z

Haigh ID, Eliot M, Pattiaratchi C (2011) Global influences of the 18.61 year nodal cycle and 8.85 year cycle of lunar perigee on high tidal levels. J Geophys Res 116:C06025. https://doi.org/10.1029/2010jc006645

Haigh ID, Wijeratne EMS, MacPherson LR, Pattiaratchi CB, Mason MS, Crompton RP, George S (2014a) Estimating present day extreme water level exceedance probabilities around the coastline of Australia: tides, extra-tropical storm surges and mean sea level. Clim Dynam 42:121–138. https://doi.org/10.1007/s00382-012-1652-1

Haigh ID, MacPherson LR, Mason MS, Wijeratne EMS, Pattiaratchi CB, Crompton RP, George S (2014b) Estimating present day extreme water level exceedance probabilities around the coastline of Australia: tropical cyclone-induced storm surges. Clim Dynam 42:139–157. https://doi.org/10.1007/s00382-012-1653-0

Haigh ID, Pickering MD, Green JAM, Arbic BK, Arns A, Dangendorf S, Hill D, Horsburgh K, Howard T, Idier D, Jay DA, Lee SB, Müller M, Schindelegger M, Talke SA, Wilmes S-B, Woodworth PL (2019) The tides they are a-changin'. Submitted to Reviews of Geophysics

Häkkinen S (2000) Decadal air-sea interaction in the North Atlantic based on observations and modelling results. J Clim 13:1195–1219. https://doi.org/10.1175/1520-0442(2000)013<1195:DASIIT>2.0.CO;2

Häkkinen S, Geiger CA (2000) Simulated low-frequency modes of circulation in the Arctic Ocean. J Geophys Res Oceans 105:6549–6564. https://doi.org/10.1029/2000JC900003

Hall A, Visbeck M (2002) Synchronous variability in the Southern Hemisphere atmosphere, sea ice, and ocean resulting from the Annular Mode. J Clim 15:3043–3057. https://doi.org/10.1175/1520-0442(2002)015<3043:SVITSH>2.0.CO;2

Hamlington BD, Leben RR, Kim K-Y, Nerem RS, Atkinson LP, Thompson PR (2015) The effect of the El Niño-Southern Oscillation on U.S. regional and coastal sea level. J Geophys Res Oceans 120:3970–3986. https://doi.org/10.1002/2014JC010602

Hamlington BD, Cheon SH, Thompson PR, Merrifield MA, Nerem RS, Leben RR, Kim K-Y (2016) An ongoing shift in Pacific Ocean sea level. J Geophys Res Oceans 121:5084–5097. https://doi.org/10.1002/2016JC011815

Han W, Vialard J, McPhaden MJ, Lee T, Masumoto Y, Feng M, de Ruijter WPM (2014) Indian Ocean decadal variability: a review. B Am Meteorol Soc 95:1679–1703. https://doi.org/10.1175/BAMS-D-13-00028.1

Han W, Meehl GA, Stammer D, Hu A, Hamlington B, Kenigson J, Palanisamy H, Thompson P (2017a) Spatial patterns of sea level variability associated with natural internal climate modes. Surv Geophys 38:217–250. https://doi.org/10.1007/s10712-016-9386-y

Han W, Meehl GA, Hu A, Zheng J, Kenigson J, Vialard J, Rajagopalan B, Yanto (2017b) Decadal variability of Indian and Pacific Walker Cells: do they co-vary on decadal timescales? J Clim 30:8447–8468. https://doi.org/10.1175/JCLI-D-16-0783.1

Han W, Stammer D, Meehl GA, Hu A, Sienz F, Zhang L (2018a) Multi-decadal trend and decadal variability of the regional sea level over the Indian Ocean since the 1960s: roles of climate modes and external forcing. Climate 6:51. https://doi.org/10.3390/cli6020051

Han W, Vialard J, McPhaden M, Roxy MK, Feng M, Shinoda T, Lee T (2018b) Regional sea-level variability and change. Chapter 14. In: Vialard J, Beal L (eds) Indian ocean observing system (IndOOS) decadal review. CLIVAR, Qingdao (in press)

Harangozo SA (1993) Flooding in the Maldives and its implications for the global sea level rise debate. In: Woodworth PL, Pugh DT, De Ronde JG, Warrick RG, Hannah J (eds) Sea level changes: determination and effects, vol 69. Geophysical monograph series. American Geophysical Union, Washington, pp 95–99. https://doi.org/10.1029/gm069

Hemer MA, Fan Y, Mori N, Semedo A, Wang XL (2013) Projected future changes in wind-wave climate in a multi-model ensemble. Nat Clim Change 3:471–476. https://doi.org/10.1038/nclimate1791

Hibbert A, Leach H, Woodworth P, Hughes CW, Roussenov V (2010) Quasi-biennial modulation of the Southern Ocean Coherent Mode. Q J R Meteor Soc 136:755–768. https://doi.org/10.1002/qj.581

Higginson S, Thompson KR, Woodworth PL, Hughes CW (2015) The tilt of mean sea level along the east coast of North America. Geophys Res Lett 42:1471–1479. https://doi.org/10.1002/2015GL063186

Hill DF (2016) Spatial and temporal variability in tidal range: evidence, causes, and effects. Curr Clim Change Rep 2:232–241. https://doi.org/10.1007/s40641-016-0044-8

Hoeke RK, McInnes KL, O'Grady J (2015) Wind and wave setup contributions to extreme sea levels at a tropical high island: a stochastic cyclone simulation study for Apia, Samoa. J Mar Sci Eng 3:1117–1135. https://doi.org/10.3390/jmse3031117

Hoeke RK, McInnes KL, Kruger JC, McNaught RJ, Hunter JR, Smithers SG (2013) Widespread inundation of Pacific islands triggered by distant-source wind-waves. Global Planet Change 108:128–138. https://doi.org/10.1016/j.gloplacha.2013.06.006

Holgate SJ, Woodworth PL (2004) Evidence for enhanced coastal sea level rise during the 1990s. Geophys Res Lett 31:L07305. https://doi.org/10.1029/2004GL019626

Holman RA, Sallenger AH Jr (1985) Setup and swash on a natural beach. J Geophys Res 90(C1):945–953. https://doi.org/10.1029/JC090iC01p00945

Holton JR, Lindzen RS (1972) An updated theory for quasi-biennial cycle of tropical stratosphere. J Atmos Sci 29:1076–1080. https://doi.org/10.1175/1520-0469(1972)029<1076:AUTFTQ>2.0.CO;2

Hughes CW, Meredith MP (2006) Coherent sea-level fluctuations along the global continental slope. Philos Trans R Soc A 364:885–901. https://doi.org/10.1098/rsta.2006.1744

Hughes CW, Stepanov VN (2004) Ocean dynamics associated with rapid J2 fluctuations: importance of circumpolar modes and identification of a coherent Arctic mode. J Geophys Res 109:C06002. https://doi.org/10.1029/2003JC002176

Hughes CW, Woodworth PL, Meredith MP, Stepanov V (2003) Coherence of Antarctic sea levels, Southern Hemisphere Annular Mode, and flow through Drake Passage. Geophys Res Lett 30:1464. https://doi.org/10.1029/2003GL017240

Hughes CW, Williams J, Blaker A, Coward A, Stepanov V (2018) A window on the deep ocean: the special value of ocean bottom pressure for monitoring the large-scale, deep-ocean circulation. Prog Oceanogr 161:19–46. https://doi.org/10.1016/j.pocean.2018.01.011

Hughes CW, Thompson K, Minobe S, Fukumori I, Griffies S, Huthnance J, Spence P (2019) Sea level and the role of coastal-trapped waves in mediating the interaction between the coast and open ocean. Surv Geophys. https://doi.org/10.1007/s10712-019-09535-x

Huthnance JM (1978) On coastal trapped waves: analysis and numerical calculation by inverse iteration. J Phys Oceanogr 8:74–92. https://doi.org/10.1175/1520-0485(1978)008<0074:OCTWAA>2.0.CO;2

Huthnance JM (1992) Extensive slope currents and the ocean-shelf boundary. Prog Oceanogr 29:161–196. https://doi.org/10.1016/0079-6611(92)90023-S

Huthnance JM (2001) Coastal trapped waves. In: Steele JH, Thorpe SA, Turekian KK (eds) Encyclopedia of ocean sciences, 1st edn. Academic Press, San Diego, pp 489–496

Huthnance JM, Mysak LA, Wang DP (1986) Coastal trapped waves. In: Mooers CNK (ed) Baroclinic processes on continental shelves, vol 3. Coastal and estuarine sciences. American Geophysical Union, Washington DC, pp 1–18. https://doi.org/10.1029/co003

Idier D, Paris F, Le Cozannet G, Boulahya F, Dumas F (2017) Sea-level rise impacts on the tides of the European Shelf. Cont Shelf Res 137:56–71. https://doi.org/10.1016/j.csr.2017.01.007

Idier D, Bertin X, Thompson P, Pickering MD (2019) Interactions between mean sea-level, tide, surge, waves and flooding: mechanisms and contributions to sea level variations at the coast. Surv Geophys (in review)

IOC (2016) Manual on sea-level measurements and interpretation, volume V: Radar Gauges. Paris, Intergovernmental Oceanographic Commission of UNESCO. 104 pp. (IOC Manuals and Guides No.14, vol. V; JCOMM Technical Report No. 89) (English). http://unesdoc.unesco.org/images/0024/002469/246981E.pdf which includes a Supplement: Practical Experiences. Accessed 1 Mar 2019

Jahfer S, Vinayachandran PN, Nanjundiah RS (2015) Long-term impact of Amazon river runoff on northern hemispheric climate. Nature 7:10989. https://doi.org/10.1038/s41598-017-10750-y

Jay DA (2009) Evolution of tidal amplitudes in the eastern Pacific Ocean. Geophys Res Lett 36:L04603. https://doi.org/10.1029/2008GL036185

Kang SK, Chung J, Lee S-R, Yum K-D (1995) Seasonal variability of the M2 tide in the seas adjacent to Korea. Cont Shelf Res 15:1087–1113. https://doi.org/10.1016/0278-4343(94)00066-V

Karpytchev M, Ballu V, Krien Y, Becker M, Goodbred S, Spada G, Calmant S, Shum CK, Khan Z (2018) Contribution of a strengthened early Holocene monsoon and sediment loading to present-day subsidence of the Ganges–Brahmaputra delta. Geophys Res Lett 45:1433–1442. https://doi.org/10.1002/2017GL076388

Kawabe M (1988) Variability of Kuroshio velocity assessed from the sea-level difference between Naze and Nishinoomote. J Oceanogr Soc Japan 44:293–304. https://doi.org/10.1007/BF02302572

Kenigson JS, Han W (2014) Detecting and understanding the accelerated sea level rise along the east coast of the United States during recent decades. J Geophys Res Oceans 119:8749–8766. https://doi.org/10.1002/2014JC010305

Kenigson JS, Han W, Rajagopalan B, Yanto Jasinski M (2018) Decadal shift of NAO-linked interannual sea level variability along the U.S. Northeast coast. J Clim 31:4981–4989. https://doi.org/10.1175/JCLI-D-17-0403.1

Kennedy AB, Mori N, Zhang Y, Yasuda T, Chen S-E, Tajima Y, Pecor W, Toride K (2016) Observations and modelling of coastal boulder transport and loading during Super Typhoon Haiyan. Coast Eng J 58:1640004–1–1640004-25. https://doi.org/10.1142/S0578563416400040

Kierulf HP, Steffen H, Simpson MJR, Lidberg M, Wu P, Wand H (2014) A GPS velocity field for Fennoscandia and a consistent comparison to glacial isostatic adjustment models. J Geophys Res Solid Earth 119:6613–6629. https://doi.org/10.1002/2013JB010889

Kirtman B, Power SB, Adedoyin JA, Boer GJ, Bojariu R, Camilloni I, Doblas-Reyes FJ, Fiore AM, Kimoto M, Meehl GA, Prather M, Sarr A, Schär C, Sutton R, van Oldenborgh GJ, Vecchi G, Wang HJ (2013) Near-term climate change: projections and predictability. In: Stocker TF, Qin D, Plattner G-K, Tignor M, Allen SK, Boschung J, Nauels A, Xia Y, Bex V, Midgley PM (eds) Climate change 2013: the physical science basis. Contribution of working group I to the fifth assessment report of the intergovernmental panel on climate change. Cambridge University Press, Cambridge, New York

Kolker AS, Allison MA, Hameed S (2011) An evaluation of subsidence rates and sea-level variability in the northern Gulf of Mexico. Geophys Res Lett 38:L21404. https://doi.org/10.1029/2011GL049458

Korosov A, Counillon F, Johannessen JA (2015) Monitoring the spreading of the Amazon freshwater plume by MODIS, SMOS, Aquarius, and TOPAZ. J Geophys Res-Oceans 120:268–283. https://doi.org/10.1002/2014JC010155

Kourafalou VH, De Mey P, Le Hénaff M, Charria G, Edwards CA, He R, Herzfeld M, Pascual A, Stanev EV, Tintoré J, Usui N, van der Westhuysen AJ, Wilkin J, Zhu X (2015) Coastal Ocean Forecasting: system integration and evaluation. J Oper Oceanogr 8(S1):s127–s146. https://doi.org/10.1080/1755876X.2015.1022336

Laiz I, Ferrer L, Plomaritis TA, Charria G (2014) Effect of river runoff on sea level from in situ measurements and numerical models in the Bay of Biscay. Deep Sea Res Pt II 106:49–67. https://doi.org/10.1016/j.dsr2.2013.12.013

Larson KM, Ray RD, Williams SDP (2017) A ten year comparison of water levels measured with a geodetic GPS receiver versus a conventional tide gauge. J Atmos Ocean Technol 34:295–307. https://doi.org/10.1175/JTECH-D-16-0101.1

LeBlond PH, Mysak LA (1978) Waves in the ocean. Elsevier Scientific Publishing, Amsterdam, p 602

Lindzen RS, Holton JR (1968) A theory of quasi-biennial oscillation. J Atmos Sci 25:1095–1107. https://doi.org/10.1175/1520-0469(1968)025<1095:ATOTQB>2.0.CO;2

Lisitzin E (1974) Sea-level changes. Elsevier, Amsterdam, p 286
Longuet-Higgins MS, Stewart RW (1962) Radiation stress and mass transport in gravity waves, with applications to "surf beats". J Fluid Mech 13:481–504. https://doi.org/10.1017/S0022112062000877
Lowe JA, Woodworth PL, Knutson T, McDonald RE, McInnes K, Woth K, Von Storch H, Wolf J, Swail V, Bernier N, Gulev S, Horsburgh K, Unnikrishnan AS, Hunter J, Weisse R (2010) Past and future changes in extreme sea levels and waves. Chapter 11. In: Church JA, Woodworth PL, Aarup T, Wilson WS (eds) Understanding sea-level rise and variability. Wiley-Blackwell, London
Lubbock JW (1836) On the tides at the port of London. Philos Trans R Soc London 126:217–266. https://doi.org/10.1098/rstl.1836.0017
Luther DS (1982) Evidence of a 4–6 day barotropic, planetary oscillation of the Pacific Ocean. J Phys Oceanogr 12:644–657. https://doi.org/10.1175/1520-0485(1982)012<0644:EOADBP>2.0.CO;2
Madden RA, Julian PR (1971) Detection of a 40–50 day oscillation in zonal wind in Tropical Pacific. J Atmos Sci 28:702–708. https://doi.org/10.1175/1520-0469(1971)028<0702:DOADOI>2.0.CO;2
Madden RA, Julian PR (1994) Observations of the 40–50-day tropical oscillation—a review. Mon Weather Rev 122:814–837. https://doi.org/10.1175/1520-0493(1994)122<0814:OOTDTO>2.0.CO;2
Madsen OS, Poon YK, Graber HC (1988) Spectral wave attenuation by bottom friction: theory. Coast Eng Proc 21:492–504. https://doi.org/10.9753/icce.v21.%25p
Mantua NJ, Hare SR (2002) The Pacific decadal oscillation. J Oceanogr 58:35–44. https://doi.org/10.1023/A:1015820616384
Marcos M, Tsimplis MN (2007) Variations of the seasonal sea level cycle in southern Europe. J Geophys Res 112:C12011. https://doi.org/10.1029/2006JC004049
Marcos M, Woodworth PL (2017) Spatio-temporal changes in extreme sea levels along the coasts of the North Atlantic and the Gulf of Mexico. J Geophys Res Oceans 122:7031–7048. https://doi.org/10.1002/2017JC013065
Marcos M, Woodworth PL (2018) Changes in extreme sea levels. CLIVAR Exch/US CLIVAR Var 16:20–24. https://doi.org/10.5065/D6445K82
Marcos M, Tsimplis MN, Shaw AGP (2009) Sea level extremes in southern Europe. J Geophys Res 114:C01007. https://doi.org/10.1029/2008JC004912
Marcos M, Calafat FM, Berihuete A, Dangendorf S (2015) Long-term variations in global sea level extremes. J Geophys Res Oceans 120:8115–8134. https://doi.org/10.1002/2015JC011173
Marcos M, Wöppelmann G, Matthews A, Ponte RM, Birol F, Ardhuin F, Coco G, Santamaría-Gómez A, Ballu V, Testut L, Chambers D, Stopa JE (2019) Coastal sea level and related fields from existing observing systems. Surv Geophys. https://doi.org/10.1007/s10712-019-09513-3
Marsooli R, Lin N (2018) Numerical modeling of historical storm tides and waves and their interactions along the U.S. east and Gulf Coasts. J Geophys Res Oceans 123:3844–3874. https://doi.org/10.1029/2017JC013434
Matthews AJ, Meredith MP (2004) Variability of Antarctic circumpolar transport and the Southern Annular Mode associated with the Madden-Julian Oscillation. Geophys Res Lett 31:L24312. https://doi.org/10.1029/2004GL021666
McCarthy GD, Smeed DA, Johns WE, Frajka-Williams E, Moat BI, Rayner D, Baringer MO, Meinen CS, Collins J, Bryden HL (2015) Measuring the Atlantic Meridional overturning circulation at 26°N. Prog Oceanogr 130:91–111. https://doi.org/10.1016/j.pocean.2014.10.006
Meade RH, Emery KO (1971) Sea level as affected by river runoff, Eastern United States. Science 173:425–428. https://doi.org/10.1126/science.173.3995.425
Melet A, Almar R, Meyssignac B (2016) What dominates sea level at the coast: a case study for the Gulf of Guinea. Ocean Dynam 66:623–636. https://doi.org/10.1007/s10236-016-0942-2
Melet A, Meyssignac B, Almar R, Le Cozannet G (2018) Under-estimated wave contribution to coastal sea-level rise. Nat Clim Change 8: 234–239. https://doi.org/10.1038/s41558-018-0088-y. Correction in Nat Clim Change 8: 840. https://doi.org/10.1038/s41558-018-0234-6
Melet A, Meyssignac B, Almar R, Le Cozannet G (2019) Reply to ''Waves do not contribute to global sea-level rise". Nat Clim Change 9:3. https://doi.org/10.1038/s41558-018-0378-4
Menéndez M, Woodworth PL (2010) Changes in extreme high water levels based on a quasi-global tide-gauge dataset. J Geophys Res 115:C10011. https://doi.org/10.1029/2009JC005997
Mentaschi L, Vousdoukas M, Voukouvalas E, Dosio A, Feyen L (2017) Global changes of extreme coastal wave energy fluxes triggered by intensified teleconnection patterns. Geophys Res Lett 44:2416–2426. https://doi.org/10.1002/2016GL072488
Meredith MP, Woodworth PL, Hughes CW, Stepanov V (2004) Changes in the ocean transport through Drake Passage during the 1980s and 1990s, forced by changes in the Southern Annular Mode. Geophys Res Lett 31:L21305. https://doi.org/10.1029/2004GL021169

Merrifield MA, Thompson PR (2018) Interdecadal sea level variations in the Pacific: distinctions between the tropics and extratropics. Geophys Res Lett 45:6604–6610. https://doi.org/10.1029/2018GL077666
Merrifield MA, Genz AS, Kontoes CP, Marra JJ (2013) Annual maximum water levels from tide gauges: contributing factors and geographic patterns. J Geophys Res 118:2535–2546. https://doi.org/10.1002/jgrc.2017
Merrifield MA, Becker JM, Ford M, Yao Y (2014) Observations and estimates of wave-driven water level extremes at the Marshall Islands. Geophys Res Lett 41:7245–7253. https://doi.org/10.1002/2014GL061005
Meyssignac B, Slangen ABA, Melet A, Church JA, Fettweis X, Marzeion B, Agosta C, Ligtenberg SRM, Spada G, Richter K, Palmer MD, Roberts CD, Champollion N (2017) Evaluating model simulations of twentieth-century sea-level rise. Part II: regional sea-level changes. J Climate 30:8565–8593. https://doi.org/10.1175/JCLI-D-17-0112.1
Middleton JF (2000) Wind-forced upwelling: the role of the surface mixed layer. J Phys Oceanogr 30:745–763. https://doi.org/10.1175/1520-0485(2000)030<0745:WFUTRO>2.0.CO;2
Middleton JF, Cirano M (1999) Wind-forced downwelling slope currents: a numerical study. J Phys Oceanogr 29:1723–1742. https://doi.org/10.1175/1520-0485(1999)029<1723:WFDSCA>2.0.CO;2
Miller GR (1972) Relative spectra of tsunamis. Hawaii Inst. Geophys Report, HIG-72-8. University of Hawaii, Hawaii
Miller L, Douglas BC (2007) Gyre-scale atmospheric pressure variations and their relation to 19th and 20th century sea level rise. Geophys Res Lett 34:L16602. https://doi.org/10.1029/2007GL030862
Miller STK, Keim BD, Talbot RW, Mao H (2003) Sea breeze: structure, forecasting, and impacts. Rev Geophys 41:1011. https://doi.org/10.1029/2003RG000124
Mitchum GT (1995) The source of 90-day oscillations at Wake Island. J Geophys Res 100(C2):2459–2475. https://doi.org/10.1029/94JC02923
Mitchum GT (2000) An improved calibration of satellite altimetric heights using tide gauge sea levels with adjustment for land motion. Mar Geod 23:145–166. https://doi.org/10.1080/01490410050128591
Monserrat S, Vilibić I, Rabinovich AB (2006) Meteotsunamis: atmospherically induced destructive ocean waves in the tsunami frequency band. Nat Hazards Earth Syst Sci 6:1035–1051. https://doi.org/10.5194/nhess-6-1035
Muis S, Verlaan M, Winsemius HC, Aerts JCJH, Ward PJ (2016) A global reanalysis of storm surge and extreme sea levels. Nat Commun 7:1–11. https://doi.org/10.1038/ncomms11969
Müller M (2012) The influence of changing stratification conditions on barotropic tidal transport and its implications for seasonal and secular changes of tides. Cont Shelf Res 47:107–115. https://doi.org/10.1016/j.csr.2012.07.003
Müller M, Arbic BK, Mitrovica JX (2011) Secular trends in ocean tides: observations and model results. J Geophys Res 116:C05013. https://doi.org/10.1029/2010JC006387
Nakanowatari T, Ohshima KI (2014) Coherent sea level variation in and around the Sea of Okhotsk. Prog Oceanogr 126:58–70. https://doi.org/10.1016/j.pocean.2014.05.009
Neetu S, Lengaigne M, Vincent EM, Vialard J, Madec G, Samson G, Ramesh Kumar MR, Durand F (2012) Influence of upper-ocean stratification on tropical cyclone-induced surface cooling in the Bay of Bengal. J Geophys Res 117:C12020. https://doi.org/10.1029/2012JC008433
Newton B, Tremblay LB, Cane MA, Schlosser P (2006) A simple model of the Arctic Ocean response to annular atmospheric modes. J Geophys Res Oceans 111:C09019. https://doi.org/10.1029/2004JC002622
Oliver ECJ, Thompson KR (2010) Madden-Julian Oscillation and sea level: local and remote forcing. J Geophys Res 115:C01003. https://doi.org/10.1029/2009JC005337
Pavlov VK (2001) Seasonal and long-term sea level variability in the marginal seas of the Arctic Ocean. Polar Res 20:153–160. https://doi.org/10.3402/polar.v20i2.6512
Pedreros R, Idier D, Muller H, Lecacheux S, Paris F, Yates-Michelin M, Dumas F, Pineau-Guillou L, Sénéchal N (2018) Relative contribution of wave setup to the storm surge: observations and modeling based analysis in open and protected environments (Truc Vert beach and Tubuai island). J Coast Res 85:1046–1050. https://doi.org/10.2112/SI85-210.1
Peltier WR, Argus DF, Drummond R (2015) Space geodesy constrains ice-age terminal deglaciation: the global ICE-6G_C (VM5a) model. J Geophys Res Solid Earth 120:450–487. https://doi.org/10.1002/2014JB011176
Pickering MD, Horsburgh KJ, Blundell JR, Hirschi JJ-M, Nicholls RJ, Verlaan M, Wells NC (2017) The impact of future sea-level rise on the global tides. Cont Shelf Res 142:50–68. https://doi.org/10.1016/j.csr.2017.02.004

Piecuch CG, Dangendorf S, Ponte RM, Marcos M (2016) Annual sea level changes on the North American northeast coast: influence of local winds and barotropic motions. J Clim 29:4801–4816. https://doi.org/10.1175/JCLI-D-16-0048.1

Piecuch CG, Bittermann K, Kemp AC, Ponte RM, Little CM, Engelhart SE, Lentz SJ (2018) River-discharge effects on United States Atlantic and Gulf coast sea-level changes. Proc Natl Acad Sci USA. https://doi.org/10.1073/pnas.1805428115 (in press)

Piecuch CG, Calafat FM, Dangendorf S, Jordà G (2019) The ability of barotropic models to simulate historical mean sea level changes from coastal tide gauge data. Surv Geophys. https://doi.org/10.1007/s10712-019-09537-9

Plag H-P, Tsimplis MN (1999) Temporal variability of the seasonal sea-level cycle in the North Sea and Baltic Sea in relation to climate variability. Global Planet Change 20:173–203. https://doi.org/10.1016/S0921-8181(98)00069-1

Poate TG, McCall RT, Masselink G (2016) A new parameterisation for runup on gravel beaches. Coast Eng 117:176–190. https://doi.org/10.1016/j.coastaleng.2016.08.003

Ponte RM et al. (2019) Towards comprehensive observing and modeling systems for monitoring and predicting regional to coastal sea level. Submitted to Front Sci

Ponte RM, Salstein DA, Rosen RD (1991) Sea level response to pressure forcing in a barotropic numerical model. J Phys Oceanogr 21:1043–1057. https://doi.org/10.1175/1520-0485(1991)021%3c1043:SLRTPF%3e2.0.CO;2

Prandi P, Cazenave A, Becker M (2009) Is coastal mean sea level rising faster than the global mean? A comparison between tide gauges and satellite altimetry over 1993–2007. Geophys Res Lett 36:L05602. https://doi.org/10.1029/2008GL036564

Proshutinsky AY, Johnson MA (1997) Two circulation regimes of the wind driven Arctic Ocean. J Geophys Res Oceans 102:12493–12514. https://doi.org/10.1029/97JC00738

Proshutinsky A, Bourke RH, McLaughlin FA (2002) The role of the Beaufort Gyre in Arctic climate variability: seasonal to decadal climate scales. Geophys Res Lett 29:L02100. https://doi.org/10.1029/2002GL015847

Proshutinsky A, Ashik IM, Dvorkin EN, Häkkinen S, Krishfield RA, Peltier WR (2004) Secular sea level change in the Russian sector of the Arctic Ocean. J Geophys Res 109:C03042. https://doi.org/10.1029/2003JC002007

Proshutinsky A, Ashik IM, Häkkinen S (2007) Sea level variability in the Arctic Ocean from AOMIP models. J Geophys Res 112:C04S08. https://doi.org/10.1029/2006jc003916

Pugh DT, Vassie JM (1976) Tide and surge propagation off-shore in the Dowsing region of the North Sea. Deutsche Hydrographische Zeitschrift 29:163–213

Pugh DT, Vassie JM (1992) Seasonal modulations of the principal semi diurnal lunar tide. In: Beven K, Chatwin P, Millbank J (eds) Mixing and transport in the environment. A memorial volume for Catherine M. Allen (1954–1991). Wiley, Chichester, pp 247–267

Pugh DT, Woodworth PL (2014) Sea-level science: Understanding tides, surges, tsunamis and mean sea-level changes. Cambridge University Press, Cambridge. ISBN 9781107028197

Qiu B, Chen S (2005) Variability of the Kuroshio Extension jet, recirculation gyre, and mesoscale eddies on decadal time scales. J Phys Oceanogr 35:2090–2103. https://doi.org/10.1175/JPO2807.1

Rabinovich AB (1997) Spectral analysis of tsunami waves: separation of source and topography effects. J Geophys Res Oceans 102:12663–12676. https://doi.org/10.1029/97JC00479

Rabinovich AB (2010) Seiches and harbor oscillations (Chapter 9). In: Kim YC (ed) Handbook of coastal engineering. World Scientific Publishing, Hackensack, pp 193–236

Rabinovich AB, Monserrat S (1996) Meteorological tsunamis near the Balearic and Kuril Islands: descriptive and Statistical analysis. Nat Hazards 13:55–90. https://doi.org/10.1007/BF00156506

Rabinovich AB, Thomson RE (2007) The 26 December 2004 Sumatra tsunami: analysis of tide gauge data from the World Ocean Part 1. Indian Ocean and South Africa. Pure appl Geophys 164:261–308. https://doi.org/10.1007/s00024-006-0164-5

Rasmussen EM, Carpenter TH (1982) Variations in tropical sea surface temperature and surface wind fields associated with the Southern Oscillation/El Niño. Mon Weather Rev 110:354–384. https://doi.org/10.1175/1520-0493(1982)110%3c0354:VITSST%3e2.0.CO;2

Raucoules D, Le Cozannet G, Wöppelmann G, de Michele M, Gravelle M, Daag A, Marcos M (2013) High nonlinear urban ground motion in Manila (Philippines) from 1993 to 2010 observed by DInSAR: implications for sea-level measurement. Remote Sens Environ 139:386–397. https://doi.org/10.1016/j.rse.2013.08.021

Ray RD (2009) Secular changes in the solar semidiurnal tide of the western North Atlantic Ocean. Geophys Res Lett 36:L19601. https://doi.org/10.1029/2009GL040217

Ray RD, Egbert GD (2017) Tides and satellite altimetry. In: Stammer D, Cazenave A (eds) Satellite altimetry over oceans and land surfaces. CRC Taylor and Francis, Boca Raton, pp 427–458

Ray RD, Egbert GD, Erofeeva SY (2011) Tide predictions in shelf and coastal waters: status and prospects. In: Vignudelli S et al (eds) Coastal altimetry. Springer, Berlin, pp 191–216. https://doi.org/10.1007/978-3-642-12796-0_8

Richter K, Nilsen JEØ, Drange H (2012) Contributions to sea level variability along the Norwegian coast for 1960–2010. J Geophys Res 117:C05038. https://doi.org/10.1029/2011JC007826

Riva REM, Frederikse T, King MA, Marzeion B, van den Broeke MR (2017) Brief communication: the global signature of post-1900 land ice wastage on vertical land motion. The Cryosphere 11:1327–1332. https://doi.org/10.5194/tc-11-1327-2017

Roden GI, Rossby HT (1999) Early Swedish contribution to oceanography: nils Gissler (1715–71) and the inverted barometer effect. B Am Meteorol Soc 80:675–682. https://doi.org/10.1175/1520-0477(1999)080%3c0675:ESCTON%3e2.0.CO;2

Roelvink D, Reniers A, van Dongeren A, van Thiel de Vries J, McCall R, Lescinski J (2009) Modelling storm impacts on beaches, dunes and barrier islands. Coast Eng 56:11–12. https://doi.org/10.1016/j.coastaleng.2009.08.006

Roemmich D, Woodworth P, Jevrejeva J, Purkey S, Lankhorst M, Send U, Maximenko N (2017) In situ observations needed to complement, validate, and interpret satellite altimetry (Chapter 3). In: Stammer D, Cazenave A (eds) Satellite altimetry over oceans and land surfaces. CRC Press, Boca Raton, pp 113–147

Ross JC (1854) On the effect of the pressure of the atmosphere on the mean level of the ocean. Philos Trans R Soc London 144:285–296. https://doi.org/10.1098/rstl.1854.0013

Roussenov VM, Williams RG, Hughes CW, Bingham RJ (2008) Boundary wave communication of bottom pressure and overturning changes for the North Atlantic. J Geophys Res 113:C08042. https://doi.org/10.1029/2007JC004501

Saji NH, Yamagata T (2003) Possible impacts of Indian Ocean Dipole Mode events on global climate. Clim Res 25:151–169

Salas-Monreal D, Valle-Levinson A (2008) Sea-level slopes and volume fluxes produced by atmospheric forcing in estuaries: chesapeake Bay case study. J Coast Res 24(Supplement 2B):208–217. https://doi.org/10.2112/06-0632.1

Sallenger AH Jr, Doran KS, Howd PA (2012) Hotspot of accelerated sea-level rise on the Atlantic coast of North America. Nat Clim Change 2:884–888. https://doi.org/10.1038/nclimate1597

Santamaría-Gómez A, Mémin A (2015) Geodetic secular velocity errors due to interanual Surface loading deformation. Geophys J Int 202:763–767. https://doi.org/10.1093/gjo/ggv190

Sasaki YN, Minobe S, Schneider N (2013) Decadal response of the Kuroshio Extension jet to Rossby waves: observation and thin-jet theory. J Phys Oceanogr 43:442–456. https://doi.org/10.1175/JPO-D-12-096.1

Sasaki YN, Minobe S, Miura Y (2014) Decadal sea-level variability along the coast of Japan in response to ocean circulation changes. J Geophys Res ceans 119:266–275. https://doi.org/10.1002/2013JC009327

Sasaki YN, Washizu R, Yasuda T, Minobe S (2017) Sea level variability around Japan during the twentieth century simulated by a regional ocean model. J Clim 30:5585–5595. https://doi.org/10.1175/JCLI-D-16-0497.1

Sella GF, Stein S, Dixon TH, Craymer M, James TS, Mazzotti S, Dokka RK (2007) Observation of glacial isostatic adjustment in "stable" North America with GPS. Geophys Res Lett 34:L02306. https://doi.org/10.1029/2006GL027081

Semedo A, Sušelj K, Rutgersson A, Sterl A (2011) A global view on the wind sea and swell climate and variability from ERA-40. J Clim 24:1461–1479. https://doi.org/10.1175/2010JCLI3718.1

Siefert W (1982) Bemerkenswerte Veränderungen der Wasserstände in den deutschen Tideflüssen. Die Küste 37: 1–36. http://www.kfki.de

Smith-Konter BR, Thornton GM, Sandwell DT (2014) Vertical crustal displacement due to interseismic deformation along the San Andreas fault: constraints from tide gauges. Geophys Res Lett 41:3793–3801. https://doi.org/10.1002/2014GL060091

Soulsby RL, Clarke S (2005) Bed shear-stresses under combined waves and currents on smooth and rough beds. HR Wallingford Report TR 137

Stammer D et al (2014) Accuracy assessment of global barotropic ocean tide models. Rev Geophys 52:243–282. https://doi.org/10.1002/2014RG000450

Stockdon HF, Holman RA, Howd PA, Sallenger AH Jr (2006) Empirical parameterization of setup, swash, and runup. Coast Eng 53:573–588. https://doi.org/10.1016/j.coastaleng.2005.12.005

Stopa JE, Cheung KF (2014) Periodicity and patterns of ocean wind and wave climate. J Geophys Res Oceans 119:5563–5584. https://doi.org/10.1002/2013JC009729

Stopa JE, Ardhuin F, Girard-Ardhuin F (2016) Wave climate in the Arctic 1992–2014: seasonality and trends. The Cryosphere 10:1605–1629. https://doi.org/10.5194/tc-10-1605-2016
Swart NC, Fyfe JC (2012) Observed and simulated changes in the Southern Hemisphere surface westerly wind-stress. Geophys Res Lett 39:L16711. https://doi.org/10.1029/2012GL052810
Sweet WV, Park J (2014) From the extreme to the mean: acceleration and tipping points of coastal inundation from sea level rise. Earth's Future 2:579–600. https://doi.org/10.1002/2014EF000272
Taguchi B, Shang-Ping X, Schneider N, Nonaka M, Sasaki H, Sasai Y (2007) Decadal variability of the Kuroshio Extension: observations and an eddy-resolving model hindcast. J Climate 20:2357–2377. https://doi.org/10.1175/JCLI4142.1
Takahashi C, Watanabe M (2016) Pacific trade winds accelerated by aerosol forcing over the past two decades. Nat Clim Change 6:768–772. https://doi.org/10.1038/nclimate2996
Talke SA, Orton P, Jay DA (2014) Increasing storm tides in New York Harbor, 1844–2013. Geophys Res Lett 41:3149–3155. https://doi.org/10.1002/2014GL059574
Tamisiea ME, Mitrovica JX (2011) The moving boundaries of sea level change: understanding the origins of geographic variability. Oceanography 24:24–39. https://doi.org/10.5670/oceanog.2011.25
Thompson KR (1980) An analysis of British monthly mean sea level. Geophys J R Astr Soc 63:57–73. https://doi.org/10.1111/j.1365-246X.1980.tb02610.x
Thompson R, Hamon BV (1980) Wave setup of harbor water levels. J Geophys Res 85:1151–1152. https://doi.org/10.1029/JC085iC02p01151
Thompson PR, Mitchum GT (2014) Coherent sea level variability on the North Atlantic western boundary. J Geophys Res Oceans 119:5676–5689. https://doi.org/10.1002/2014JC009999
Thompson DWJ, Wallace JM (1998) The Arctic Oscillation signature in the wintertime geopotential height and temperature fields. Geophys Res Lett 25:1297–1300. https://doi.org/10.1029/98GL00950
Thompson PR, Merrifield MA, Wells JR, Chang CM (2014) Wind-driven coastal sea level variability in the Northeast Pacific. J Climate 27:4733–4751. https://doi.org/10.1175/JCLI-D-13-00225.1
Törnqvist TE, Wallace DJ, Storms JEA, Wallinga J, van Dam RL, Blaauw M, Deksen MS, Klerks CJW, Meijneken C, Snijders EMA (2008) Mississippi Delta subsidence primarily caused by compaction of Holocene strata. Nat Geosci 1:173–176. https://doi.org/10.1038/ngeo129
Torres RR, Tsimplis MN (2012) Seasonal sea level cycle in the Caribbean Sea. J Geophys Res 117:C07011. https://doi.org/10.1029/2012JC008159
Tsimplis MN, Woodworth PL (1994) The global distribution of the seasonal sea level cycle calculated from coastal tide gauge data. J Geophys Res 99:16031–16039. https://doi.org/10.1029/94JC01115
UKHO (2017) Admiralty Tide Tables (including Tidal Stream Tables). NP204, Taunton, United Kingdom Hydrographic Office
Usui N, Tsujino H, Nakano H, Fujii Y, Kamachi M (2011) Decay mechanism of the 2004/05 Kuroshio large meander. J Geophys Res 116:C10010. https://doi.org/10.1029/2011JC007009
Veit E, Conrad CP (2016) The impact of groundwater depletion on spatial variations in sea level change during the past century. Geophys Res Lett 43:3351–3359. https://doi.org/10.1002/2016GL068118
Vetter O, Becker JM, Merrifield MA, Pequignet A-C, Aucan J, Boc SJ, Pollock CE (2010) Wave setup over a Pacific Island fringing reef. J Geophys Res 115:C12066. https://doi.org/10.1029/2010JC006455
Vignudelli S, Kostianoy A, Cipollini P, Benveniste J (eds) (2011) Coastal altimetry. Springer, Berlin
Vilibić I, Šepić J (2017) Global mapping of nonseismic sea level oscillations at tsunami timescales. Sci Rep 7:40818. https://doi.org/10.1038/srep40818
Vinogradov SV, Ponte RM (2010) Annual cycle in coastal sea level from tide gauges and altimetry. J Geophys Res 115:C04021. https://doi.org/10.1029/2009JC005767
Vinogradov SV, Ponte RM (2011) Low-frequency variability in coastal sea level from tide gauges and altimetry. J Geophys Res 116:C07006. https://doi.org/10.1029/2011JC007034
Vinogradov SV, Ponte RM, Heimbach P, Wunsch C (2008) The mean seasonal cycle in sea level estimated from a data-constrained general circulation model. J Geophys Res 113:C03032. https://doi.org/10.1029/2007JC004496
Vitousek S, Barnard PL, Fletcher CH, Frazer N, Erikson L, Storlazzi CD (2017) Doubling of coastal flooding frequency within decades due to sea-level rise. Sci Rep 7:1399. https://doi.org/10.1038/s41598-017-01362-7
von Storch H, Woth K (2008) Storm surges: perspectives and options. Sustain Sci 3:33–43. https://doi.org/10.1007/s11625-008-0044-2
Wahl T, Chambers DP (2015) Evidence for multidecadal variability in US extreme sea level records. J Geophys Res Oceans 120:1527–1544. https://doi.org/10.1002/2014JC010443
Wahl T, Chambers DP (2016) Climate controls multidecadal variability in U. S. extreme sea level records. J Geophys Res Oceans 121:1274–1290. https://doi.org/10.1002/2015JC011057

Wahl T, Calafat FM, Luther ME (2014) Rapid changes in the seasonal sea level cycle along the US Gulf coast from the late 20th century. Geophys Res Lett 41:491–498. https://doi.org/10.1002/2013GL058777

Wakelin SL, Woodworth PL, Flather RA, Williams JA (2003) Sea-level dependence on the NAO over the NW European Continental Shelf. Geophys Res Lett 30:1403. https://doi.org/10.1029/2003GL017041

Walter RK, Reid EC, Davis KA, Armenta KJ, Merhoff K, Nidzieko NJ (2017) Local diurnal wind-driven variability and upwelling in a small coastal embayment. J Geophys Res Oceans 122:955–972. https://doi.org/10.1002/2016JC012466

Waterhouse AF, Valle-Levinson A (2010) Transverse structure of subtidal flow in a weakly stratified subtropical tidal inlet. Cont Shelf Res 30:281–292. https://doi.org/10.1016/j.csr.2009.11.008

White NJ, Church JA, Gregory JM (2005) Coastal and global averaged sea level rise for 1950 to 2000. Geophys Res Lett 32:L01601. https://doi.org/10.1029/2004GL021391

White NJ, Haigh ID, Church JA, Koen T, Watson CS, Pritchard TR, Watson PJ, Burgette RJ, McInnes KL, You Z-J, Zhang X, Tregoning P (2014) Australian sea levels—trends, regional variability and influencing factors. Earth Sci Rev 136:155–174. https://doi.org/10.1016/j.earscirev.2014.05.011

Wiegel RL (1964) Tsunamis, storm surges, and harbor oscillations. Chapter 5 in Oceanographical engineering. Prentice-Hall, Englewood Cliffs, pp 95–127

Wijeratne EMS, Woodworth PL, Stepanov VN (2008) The seasonal cycle of sea level in Sri Lanka and Southern India. Western Indian Ocean J Mar Sci 7:29–43. https://doi.org/10.4314/wiojms.v7i1.48252

Wijeratne EMS, Woodworth PL, Pugh DT (2010) Meteorological and internal wave forcing of seiches along the Sri Lanka coast. J Geophys Res 115:C03014. https://doi.org/10.1029/2009JC005673

Williams J, Hughes CW (2013) The coherence of small island sea level with the wider ocean: a model study. Ocean Sci 9:111–119. https://doi.org/10.5194/os-9-111-2013

Wilson B (1972) Seiches. Adv Hydrosci 8:1–94. https://doi.org/10.1016/B978-0-12-021808-0.50006-1

Wolf J (1999) The estimation of shear stresses from near-bed turbulent velocities for combined wave–current flows. Coast Eng 37:529–543. https://doi.org/10.1016/S0378-3839(99)00042-3

Woodworth PL (2010) A survey of recent changes in the main components of the ocean tide. Cont Shelf Res 30:1680–1691. https://doi.org/10.1016/j.csr.2010.07.002

Woodworth PL (2012) A note on the nodal tide in sea level records. J Coast Res 28:316–323. https://doi.org/10.2112/JCOASTRES-D-11A-00023.1

Woodworth PL (2018) Sea level change in Great Britain between 1859 and the present. Geophys J Int 213:222–236. https://doi.org/10.1093/gji/ggx538

Woodworth PL, Windle SA, Vassie JM (1995) Departures from the local inverse barometer model at periods of 5 days in the central South Atlantic. J Geophys Res 100:18281–18290. https://doi.org/10.1029/95JC01741

Woodworth PL, Hughes CW, Blackman DL, Stepanov VN, Holgate SJ, Foden PR, Pugh JP, Mack S, Hargreaves GW, Meredith MP, Milinevsky G, Fierro Contreras JJ (2006) Antarctic peninsula sea levels: a real time system for monitoring Drake Passage transport. Antarct Sci 18:429–436. https://doi.org/10.1017/S0954102006

Woodworth PL, Flather RA, Williams JA, Wakelin SL, Jevrejeva S (2007) The dependence of UK extreme sea levels and storm surges on the North Atlantic Oscillation. Cont Shelf Res 27:935–946. https://doi.org/10.1016/j.csr.2006.12.007

Woodworth PL, Pugh DT, Bingley RM (2010) Long term and recent changes in sea level in the Falkland Islands. J Geophys Res 115:C09025. https://doi.org/10.1029/2010JC006113

Woodworth PL, Menéndez M, Gehrels WR (2011) Evidence for century-timescale acceleration in mean sea levels and for recent changes in extreme sea levels. Surv Geophys 32:603–618. https://doi.org/10.1007/s10712-011-9112-8 (erratum page 619)

Woodworth PL, Morales Maqueda MÁ, Roussenov VM, Williams RG, Hughes CW (2014) Mean sea-level variability along the northeast American Atlantic coast and the roles of the wind and the overturning circulation. J Geophys Res Oceans 119:8916–8935. https://doi.org/10.1002/2014JC010520

Woodworth PL, Morales Maqueda MÁ, Gehrels WR, Roussenov V, Williams RG, Hughes CW (2017a) Variations in the difference between mean sea level measured either side of Cape Hatteras and their relation to the North Atlantic Oscillation. Clim Dynam 49:2451–2469. https://doi.org/10.1007/s00382-016-3464-1

Woodworth PL, Wöppelmann G, Marcos M, Gravelle M, Bingley RM (2017b) Why we must tie satellite positioning to tide gauge data. Eos Trans Am Geophys Union 98(4): 13–15. https://doi.org/10.1029/2017eo064037, https://eos.org/opinions/why-we-must-tie-satellite-positioning-to-tide-gauge-data

Wöppelmann G, Marcos M (2016) Vertical land motion as a key to understanding sea level change and variability. Rev Geophys 54:64–92. https://doi.org/10.1002/2015RG000502
World Meteorological Organization (2011) Guide to Storm Surge Forecasting. WMO Report No. 1076. Geneva: World Meteorological Organization. https://library.wmo.int. Accessed 14 Apr 2019
Wunsch C, Gill AE (1976) Observations of equatorially trapped waves in Pacific sea level variations. Deep Sea Res Oceanogr Abstr 23:371–390. https://doi.org/10.1016/0011-7471(76)90835-4
Wunsch C, Stammer D (1997) Atmospheric loading and the oceanic "inverted barometer" effect. Rev Geophys 35:79–107. https://doi.org/10.1029/96RG03037
Xie PP, Arkin PA (1997) Global precipitation: a 17-year monthly analysis based on gauge observations, satellite estimates, and numerical model outputs. B Am Meteorol Soc 78:2539–2558. https://doi.org/10.1175/1520-0477(1997)078%3c2539:GPAYMA%3e2.0.CO;2
Yasuda T, Sakarai K (2006) Interdecadal variability of the sea surface height around Japan. Geophys Res Lett 33:L01605. https://doi.org/10.1029/2005GL024920
Yin J, Goddard PB (2013) Oceanic control of sea level rise patterns along the East Coast of the United States. Geophys Res Lett 40:5514–5520. https://doi.org/10.1002/2013GL057992
Yin JJ, Schlesinger ME, Stouffer RJ (2009) Model projections of rapid sea level rise on the northeast coast of the United States. Nat Geosci 2:262–266. https://doi.org/10.1038/ngeo462
Young IR (1999) Seasonal variability of the global ocean wind and wave climate. Int J Climatol 19:931–950. https://doi.org/10.1002/(SICI)1097-0088(199907)19:9%3c931:AID-JOC412%3e3.0.CO;2-O
Young IR, Zieger S, Babanin AV (2011) Global trends in wind speed and wave height. Science 332:451–455. https://doi.org/10.1126/science.1197219
Zhang C (2005) Madden-Julian oscillation. Rev Geophys 43:RG2003. https://doi.org/10.1029/2004RG000158
Zhao Z, Alford MH, Girton JB, Rainville L, Simmons HL (2016) Global observations of open-ocean mode-1 M2 internal tides. J Phys Oceanogr 46:1657–1684. https://doi.org/10.1175/JPO-D-15-0105.s1
Zhuang W, Qiu B, Du Y (2013) Low-frequency western Pacific Ocean sea level and circulation changes due to the connectivity of the Philippine Archipelago. J Geophys Res Oceans 118:6759–6773. https://doi.org/10.1002/2013JC009376